Technische Universität München
TUM School of Medicine and Health

Functional reorganization of language function in glioma patients on cortical and subcortical levels as measured by navigated repetitive transcranial magnetic stimulation

Lara Anabel Engel

Vollständiger Abdruck der von der TUM School of Medicine and Health der Technischen Universität München zur Erlangung einer Doktorin der Medizin (Dr. med.) genehmigten Dissertation.

Vorsitz: Prof. Dr. Florian Eyer

Prüfende der Dissertation:

1. apl. Prof. Dr. Sandro M. Krieg
2. Priv.-Doz. Dr. Vicki Butenschön

Die Dissertation wurde am 11.04.2024 bei der Technischen Universität München eingereicht und durch die TUM School of Medicine and Health am 07.08.2024 angenommen.

Für meine Familie

Für Sibylle

Für Martin

TABLE OF CONTENTS

LIST OF FIGURES

LIST OF TABLES

1. INTRODUCTION

1.1. Anatomical language organization

1.1.1. Classic models

In the past, a living human's skull resembled a black box. While the inputting stimulus and the outputting response were apparent, there was no possibility of observing a brain during its thought processes. Pathologic lesion studies were the only way to link different brain regions to their specific function. If a living human being showed a permanent cognitive deficit and a brain lesion was later discovered in the postmortal dissection (e.g., bleeding, stroke, infection, tumor), it could be inferred that the damaged brain region was the cause of the cognitive disorder.

In this manner, the two famous scientists Paul Broca and Carl Wernicke examined the origins of speech in the 19th century. In 1861, Paul Broca published the case of Monsieur Tan, a patient who suffered from a progressive loss of speech. The only syllable he could pronounce was "tan". Nevertheless, his speech comprehension appeared to be unimpaired. In Tan's postmortal autopsy, Broca found a lesion in the left frontal lobe (Broca, 1861a, b). In the years that followed, Broca pursued this line of research and published a study that included twelve patients suffering from symptoms similar to Monsieur Tan. The results of the postmortal dissections indicated to Broca that all of their lesions affected the opercular and triangular parts of the left inferior frontal lobe. Thus, he concluded production of speech must arise from this area (Berker et al., 1986). Since then, this region has been known as the Broca's area, and the corresponding symptom complex, an expressive and non-fluent language impairment, has been called Broca's aphasia.

Two decades later, Carl Wernicke published "The aphasic symptom complex: a psychological study from an anatomical basis" (Wernicke, 1874). It was also a lesion study based on the research of his mentor, Theodor Meynert, concerning the mapping of subcortical pathways in dissected brains (Whitaker and Etlinger, 1993). In his work, Wernicke gathered cases suffering from fluent aphasia that lacked content. His patients had lost the ability to understand spoken or written language. Although they could speak and write, these functions were rather meaningless. In their postmortal dissection, he found lesions in the superior temporal gyrus (STG). Thus, he suspected speaking comprehension was located in this region, today known as the Wernicke's area. Therefore, he distinguished between Broca's motor aphasia and Wernicke's sensory, or receptive, aphasia.

Furthermore, Wernicke described the case of a patient suffering from another type of language disorder. While being able to speak fluently and having no impairment of auditory comprehension, this patient was unable to repeat spoken words. Postmortem, perisylvian

lesions were found, which affected neither Broca's nor Wernicke's area. Thus, Wernicke concluded there were fibers connecting the two areas, and damage would lead to this kind of conduction aphasia. (Wilkins and Brody, 1970). In 1822, his hypothesis was studied and supported by Carl Friedrich Burdach, a German physiologist who named this bundle of fibers *Fasciculus arcuatus* (arcuate fascicle (AF)) based on their shape (Burdach, 1822).

Wernicke's language model was adopted and refined by Norman Geschwind in the 1960s. In addition to Broca's and Wernicke's area, he integrated more regions of the brain into the model to explain different skills related to language processing (e.g., speech comprehension, speaking, reading, and writing). Today, this model is known as the Wernicke-Geschwind model.

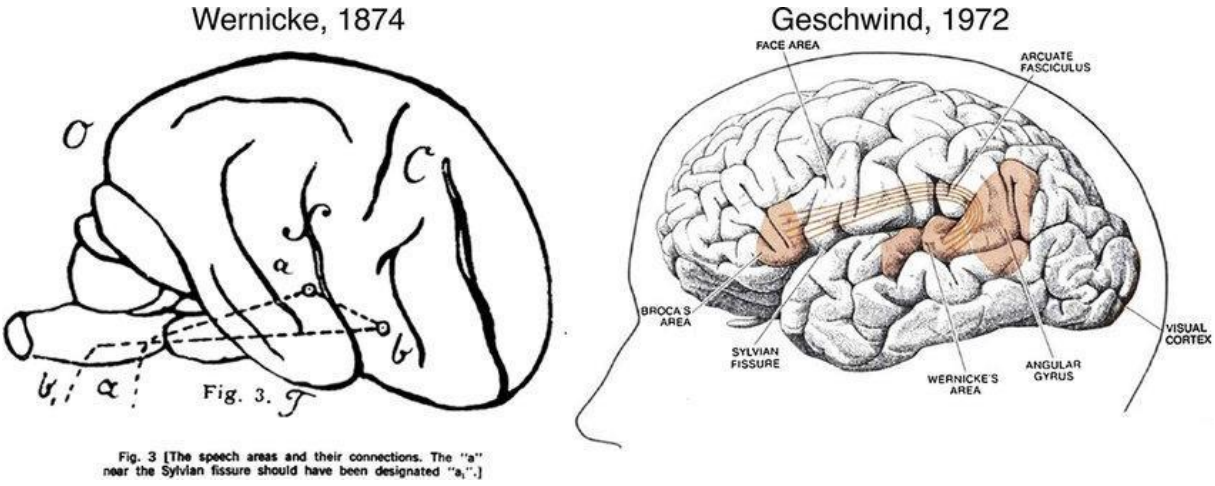

Figure 1 *Wernicke model and Geschwind model*

Left: The original model from Wernicke, 1874. For unknown reasons, the model is represented on the right hemisphere, although Wernicke's patients had lesions on the left hemisphere. Right: An update of the classic model from Geschwind, 1972. In this figure, according to most anatomical definitions, the superior temporal gyrus is inadvertently mislabeled as the angular gyrus (Tremblay and Dick, 2016).

Images used with permission from Prof. Pascale Tremblay, Ph.D. and Elsevier.

1.1.2. Dual stream model of language

Neuro-oncological experience has shown that previously established functional areas, such as Broca's and Wernicke's region, are resectable without causing any impairment (Duffau, 2014, 2018). Modern techniques of examining living brains have proven that language is not limited to specific cortical areas. Instead, language extends to extensive subcortical white-matter pathways, suggesting that language is delocalized and dynamic, that plasticity develops over time and differences between individuals exist. This multidimensional approach was labeled as *hodotopical* by Hugue Duffau, a professor in the neurosurgery department at the Montpellier University Medical Center. This term is a morphology of the words hodological (the study of

interconnections of neurons, also known as connectomics) and topological (the study of structures that keep their shape despite continuous deformation) (De Benedictis and Duffau, 2011; Duffau et al., 2014). A reexamination of the preserved brains of Broca's first two patients using high-resolution magnetic resonance imaging (MRI) scans showed lesions not only affecting cortical areas but also reaching deeper into subcortical pathways (Dronkers et al., 2007). The most accepted explanation for this complex cortical-subcortical interaction is the *dual stream model of language*, established by the scientists Hickok & Poeppel (Hickok and Poeppel, 2004) and, although slightly different, by Rauschecker and Scott (Rauschecker and Scott, 2009). These scientists proposed the following system of speech processing: Acoustic information is analyzed in the auditory cortices and then carried forward by two different streams. A *ventral semantic stream* is involved in speech recognition and comprehension. This stream unites the inferior longitudinal fascicle (ILF), the inferior fronto-occipital fasclicle (IFOF), and the uncinate fascicle (UF). Because it runs through the external capsule, it connects the cortical areas of all the large cerebral lobes (frontal, temporal, parietal, and occipital) (Moritz-Gasser et al., 2013). This stream can be described as the *form-to-meaning pathway* (Fridriksson et al., 2016). Disturbances in the ventral stream result in semantic paraphrasia. The second stream, the *dorsal phonological stream*, is involved in articulatory sensimotoric integration. In other words, it is responsible for maintaining and acquiring language skills. It is also known as the *form-to-articulation pathway* (Fridriksson et al., 2016). This stream consists of the AF and parts of the superior longitudinal fascicle (SLF). It runs around the sylvian fissure and connects the posterior frontal lobe with perisylvian areas of the parietal and temporal lobes. Lesions affecting this stream cause misarticulation and phonemic paraphrasia (Chang et al., 2015) (Duffau et al., 2014; Hickok and Poeppel, 2004, 2007).

The dual stream model has been augmented by a newly discovered stream, the frontal aslant tract (FAT). Research suggests it is involved in initiating and driving spontaneous speech (Fujii et al., 2015).

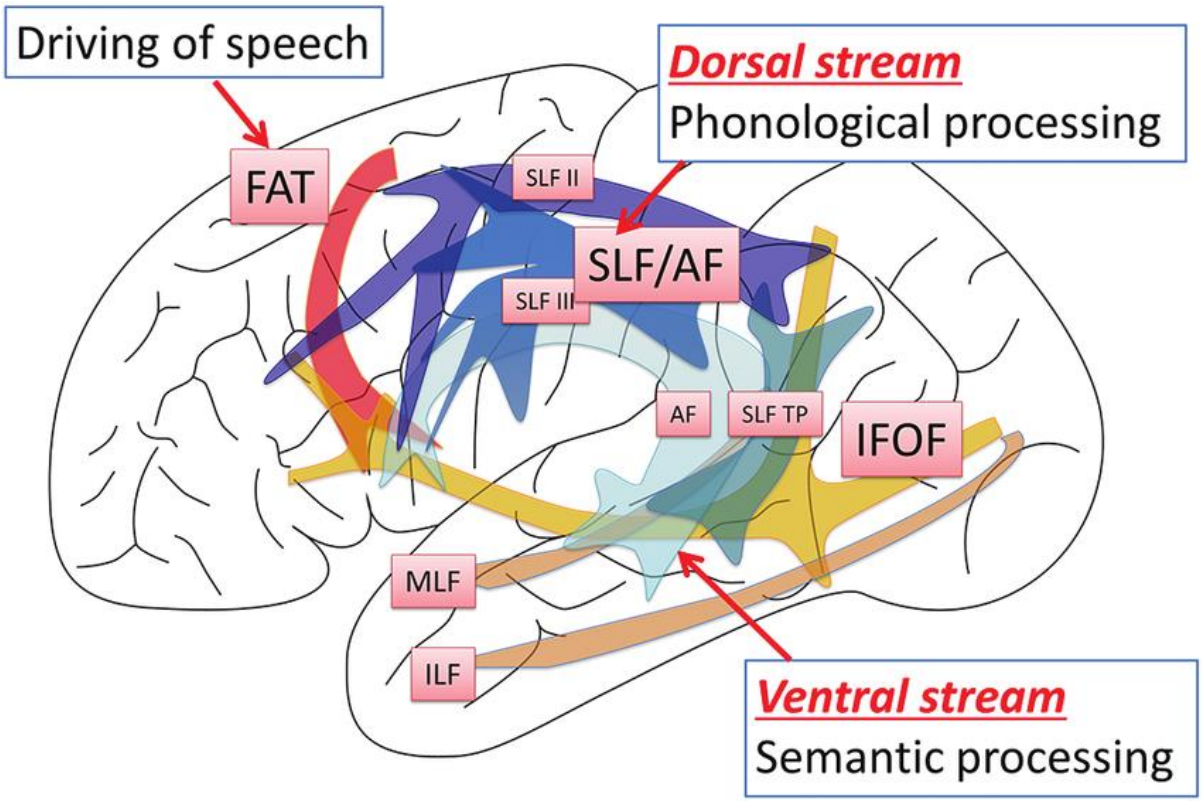

Figure 2 *Dual stream model of language as proposed by Hickok and Poeppel*
The dorsal phonological stream consists of the arcuate fascicle (AF) and the superior longitudinal fascicle (SLF). It is involved in articulatory sensimotoric integration. The ventral semantic stream unites the inferior longitudinal fascicle (ILF), the inferior fronto-occipital fasclicle (IFOF), and the uncinate fascicle (UF). It is responsible for speech recognition and comprehension. The frontal aslant tract (FAT) initiates spontaneous speech (Hickok and Poeppel, 2004).
(Fujii et al., 2016). Image used with permission from the Japan Neurosurgical Society.

1.2. Lateralization of language function

Different brain functions are distributed across both hemispheres in different ways. For instance, visual, motor, or sensory functions are located in comparable areas bilaterally. In contrast, language function is typically more pronounced in the left hemisphere. This phenomenon of functional asymmetry is called lateralization.

1.2.1. Examining hemispheric dominance

There are different approaches for measuring lateralization. Apart from the aforementioned lesion studies (particularly acute stroke cases), both invasive and non-invasive techniques are used to distinguish left- and right-hemispheric activity.
Research on lateralization began with examining so-called split-brain patients who had been treated for refractory epilepsy by a surgical corpus callosotomy. From these cases, left- and

right-side hemispheric activity became distinguishable due to elaborate examination setups. In 1981, the neurobiologist Roger Sperry won the Nobel Prize in Physiology or Medicine. His thesis stated that while the left hemisphere is analytical and executive and able to calculate, write, and speak, the right hemisphere, although mute, is superior in interpreting auditory impressions and analyzing complex relationships (Sperry, 1974).

These studies could be pursued more intensively by using data from patients who underwent the Wada test, a reversible corpus callosotomy by a very distinctive use of anesthesia (Abou-Khalil, 2007; Magee et al., 2012; Wada and Rasmussen, 2007). The test is performed to prepare patients for epilepsy surgery. Due to its invasiveness, it is not solely performed for research purposes.

Today, there are non-invasive examination techniques. Although these techniques do not only permit a hemispheric allocation, they enable the connection of a mental process to its executing cortical area. Functional magnetic resonance imaging (fMRI) is certainly the most ubiquitous of these methods (Charles et al., 1994). Repetitive transcranial magnetic stimulation language mapping (Ille et al., 2016) and magnetoencephalography (MEG) (Findlay et al., 2012) are just as effective as fMRI; however, they are less accessible.

1.2.2. Left hemispheric language dominance

Paul Broca's aphasic patients suffered exclusively from left-sided lesions. His findings gave birth to the idea that language function was limited solely to the brain's left hemisphere. The concept of functional asymmetry of language function was born. Later on, also morphological differences were found. The mean volume of the left-sided Broca's area is slightly larger than its right-sided equivalent (Toga and Thompson, 2003).

All of the aforementioned examination methods confirmed a left-sided language dominance. However, contrary to initial assumptions, all of these methods, including direct electrical stimulation (DES) during awake surgery, also detected language function in the brain's right hemisphere. Thus, researchers concluded that speech processing was a bilateral action (Baum et al., 2012; Chang et al., 2011; Duffau et al., 2008a; Sollmann et al., 2014; Szaflarski et al., 2002).

Another prominent finding was that the extent of an individual's right-hemispheric language function varies depending on whether that individual is right- or left-handed. Most humans are right-handed (around 85%–90%), having a language-dominant left hemisphere. Additionally, right-hemispheric language dominance increases as left-handedness increases, from 4% in strong right-handers to 27% in strong left-handers (Knecht et al., 2000). Since language dominance in the right hemisphere is rare, only a few data exist regarding its organization. A direct DES study that included patients with right-hemispheric language function (as detected by the Wada test) undergoing right-sided perisylvian surgery suggested that their language

networks are organized exactly inversely to people with left-hemispheric language dominance (Chang et al., 2011).

1.3. Mapping of language function

1.3.1. Direct electrical stimulation

In the late 19th century, the two German scientists Gustav T. Fritsch and Eduard Hitzig developed the idea of electrically stimulating a living brain. In their experiments on dogs, they were able to prove that different functions are located in different cortical areas (Fritsch, 1870). Another 50 years passed until this technique was applied to patients. The Canadian neurosurgeon Wilder Penfield is known as the pioneer of DES. He invented the Montreal procedure to treat patients with severe epilepsy. During an awake craniotomy, he identified the cortical epileptic focus via electrical stimulation and removed it surgically. Simultaneously, he utilized these cases to gather information on the localization of different functions. Finally, he was able to introduce the two famous cortical homunculi—one for the primary sensory cortex and one for the primary motor cortex (Penfield and Boldrey, 1937). Penfield utilized DES to locate language eloquent areas to spare these areas during surgery, among other things (Penfield and Rasmussen, 1949). By doing so, he was able to confirm observations of previous lesion studies. Penfield stated that language was mainly located in the brain's left hemisphere, even in left-handed patients, and that language function was especially dependent on subcortical structures (Penfield and Roberts, 1959).

DES soon became a clinical standard. These findings were significant for epilepsy patients who were formerly considered inoperable if their focus was located in the central parts of the left hemisphere. Resections in these areas had frequently caused aphasia, as language function is not just bundled in one specific area; it is widespread and varies significantly between individuals (Ojemann and Whitaker, 1978).

Today, direct cortical stimulation (DCS) during awake craniotomy is still the gold standard for identifying eloquent cortical areas when resecting language eloquent gliomas. This technique maximizes the extent of tumor resection while minimizing permanent language deficits (Haglund et al., 1994).

1.3.2. Transcranial electric stimulation

A new approach to brain stimulation was utilized in 1980. A group of scientists had succeeded in electrically stimulating the brain noninvasively. They did not need to penetrate the skull, the former stimulation barrier. By the use of very brief, high voltage shocks, they managed to activate a motor reaction while simultaneously making the procedure bearable for the person being tested. The era of virtual lesion studies was born (Merton and Morton, 1980).

1.3.3. Transcranial magnetic stimulation

A few years later, in 1985, an examination technique called transcranial magnetic stimulation (TMS) was introduced in the *Lancet*. By using magnetic stimulation rather than electrical, direct contact between the scalp and the electrodes was no longer needed, and discomfort was thus minimized. Moreover, the skull no longer constituted a barrier that was only surmountable by forceful stimulation since a magnetic field passes through high-resistance structures especially well (Barker et al., 1985).

Similar to DES in its beginning, research on TMS concentrated on the primary motor cortex at first, as successful stimulations can be detected easily by the conduction of motor evoked potentials (MEP) (Barker et al., 1987).

Another significant breakthrough was the combination of TMS with a navigational system, resulting in the nTMS (navigated transcranial magnetic stimulation) technique. Until nTMS was developed, TMS mapping had been conducted by using anatomical landmarks. Now the key innovation was the addition of a stereotactic navigational system that was originally created for intraoperative use. The system was able to virtually align the test person and corresponding MRI in three-dimensional (3D) space, enabling very precise stimulation (Ettinger et al., 1998; Ruohonen and Karhu, 2010).

In 1991, Alvaro Pascual-Leone, a professor at Harvard Medical School, pursued his vision of mapping language function. He was the first person to report on reproducible speech arrests in epileptic patients using the rapid-rate TMS (rTMS) technique; a stimulation method with high frequency pulses (Pascual-Leone et al., 1991).

Different researchers adopted his idea. In the following years, it was repeatedly verified that TMS was indeed able to locate cortical language function (Devlin and Watkins, 2007).

Even though there was a consensus on the functionality of language mapping by TMS, the execution of this process varied among clinical centers (Hamberger, 2007). Part of the problem was that language mapping produced various disruptions or negative effects. Compared to TMS motor mapping, which leads to positive muscle contractions, a lack of language performance using the rTMS technique is much harder to assess.

In 2009, a committee of scientists assembled to close this gap and standardize the technique. The guidelines they formulated for TMS addressed safety, ethical, and legal issues, among others (Rossi et al., 2009). These guidelines are still valid today.

Clinically, DES has been in use for decades and nTMS for only a few years. These mapping methods proved extremely beneficial to the outcomes of short- and long-term glioma patients. Patients who have undergone brain mapping during surgery have had substantially larger resections and fewer late, severe neurologic deficits (De Witt Hamer et al., 2012; Frey et al., 2014).

Furthermore, the scope of application is steadily growing. The TMS technique is used in research and in clinical practice, as an examination or a therapeutic tool.

1.3.4. Functional magnetic resonance imaging

Although the use of nTMS is growing steadily, fMRI is still the non-invasive standard tool used for presurgical planning (FitzGerald et al., 1997). It is able to detect neuronal activity by changes in cerebral blood flow. The blood oxygen level-dependent (BOLD) contrast remains the oldest, most common form of fMRI. It was introduced in 1990, and it uses hemoglobin as an endogenous contrast medium by using the different magnetic capacities of oxygenated and deoxygenated hemoglobin. Activated brain areas show an increase in metabolism and therefore have a higher turnover of oxygenated hemoglobin. In the resulting image stack, these areas are color-coded (Ogawa et al., 1990).

Eloquent areas are activated as the patient undergoes an object-naming task, allowing for the mapping of language.

Even though fMRI results are not perfectly replicable, they are a ubiquitous tool for in vivo investigations of brain function (Bennett and Miller, 2010).

Compared to other techniques, fMRI has proven to be less sensitive than DCS but more specific than rTMS. Therefore, a combination of the two non-invasive techniques is suggested (Ille et al., 2015b).

1.3.5. White-matter pathway tractography

A complete depiction of an individual language network includes not only cortical language sites but also their connecting subcortical pathways. This is especially important for presurgical planning issues, as even small damage to white-matter pathways can lead to permanent functional impairments. Diffusion tensor imaging (DTI) fiber tracking (FT) has become a common technique to fulfill this task.

1.3.5.1. DTI

A DTI MRI allows for *in vivo* white matter tractography. As a subtype of diffusion-weighed MRI (DWI), DTI MRI displays the directed diffusion of water molecules along subcortical fibers (Basser et al., 1994).

Like an MRI, a DTI sequence is subdivided into little cubes by a three-dimensional grid. The smallest units are called voxels. For every voxel, two qualities are determined: the rate of diffusion and the main direction of diffusion. From these values, a tensor is calculated. The tensor is an equation that characterizes the three-dimensional manner of water diffusion. As axons have a tubular shape, water molecules diffuse faster from one end to the other longitudinally than transversely. This directed form of diffusion along one vector is labeled “anisotropic.” In contrast, an even diffusion in every direction is called “isotropic” (Beaulieu and

Allen, 1994). Since white-matter tracts are nothing more than bundles of parallel arranged axons, their vectors add up, and a DTI tractography can display them.

1.3.5.2. Diffusion tensor imaging fiber tracking (DTI FT)

Alone, a DTI sequence has one major limitation. Because it follows voxels facing in the same direction and strung together instead of individual axons, it cannot differentiate between tracts nor deal with intersecting pathways. A subsequent DTI fiber tracking is able to provide a remedy, as it facilitates a virtual dissection of different white-matter pathways. Currently, there are numerous FT software available. Fundamentally, a distinction is made between two different kinds of algorithms:

- **Deterministic algorithms:**
  Once given a starting point, this algorithm follows the diffusion tensors from one voxel to another to reconstruct fibers. The result is a fairly overwhelming tractography, as along with the desired large white matter pathways many small fibers are tracked.
- **Probabilistic algorithms:**
  These algorithms follow a different approach. They do not use DTI tensors. Instead, these algorithms calculate the probability of connections between certain areas of the brain. With the help of a probability-density function, the likelihood of an aimed fiber orientation is calculated for every voxel. With this information, a FT is performed. Unfortunately, this approach takes a lot of time and processing power. Thus, it is less suitable for clinical practice.

Regardless of the chosen algorithm, every FT software demands the definition of regions of interest (ROIs). These are fixed points that fibers need to pass through.
One way of determining ROIs is by using anatomical landmarks. This approach works well in healthy test persons but has been proven unreliable in patients suffering from brain lesions. In patients with brain lesions, parts of their brain may have already perished or been shifted by lesions or edema. Additionally, lesions induce plasticity; therefore, functional areas may have already undergone relocation. In these cases, functional data are a good alternative for ROI seeding. This data can be provided by fMRI, MEG, or nTMS. However, fMRI and MEG are less suitable than nTMS data. On the one hand, MEG diagnostics are available in only a few departments. On the other hand, fMRI data were found to be partially falsified in brain tumor patients. It has been proven that people suffering from gliomas experience changes in intracranial oxygen levels that distort the fMRI technique (Giussani et al., 2010).

1.3.5.3. nTMS based DTI FT

The use of nTMS data in FT is currently a promising method. In this technique, cortical areas that have been determined to be electrophysiologically functional during the mapping are used as ROIs in the FT. Former studies have shown that this technique provides more reliable and detailed results than the standard DTI-FT. Feasibility has been proven concerning the use of nTMS mapped motor eloquent areas to track the corticospinal tract. Furthermore, using ROIs from data gained by navigated repetitive transcranial magnetic stimulation (nrTMS) language mapping has proven to be especially well-suited for visualizing language-related fiber tracts (Negwer et al., 2017a; Negwer et al., 2017b; Raffa et al., 2016).

One point of criticism was that inaccuracies might occur due to brain shifts. However, by using an intraoperative MRI-based elastic fusion to compensate for possible brain shifts, this assumption was refuted in a recent study. The study concluded that the severity of brain shifts was considerably overestimated in the past (Ille et al., 2021).

1.3.5.4. Intraoperative tractography during awake surgery

Similar to the gold standard DCS, intraoperative tractography has become an efficient tool for sparing white matter pathways (WMPs) during the resection of glioma. This technique can provide a real-time anatomofunctional map of specific subcortical WMPs (Duffau et al., 2008b). Recent studies have proven that its use shortens the time of awake neuro-oncological surgeries. Furthermore, intraoperative tractography could support a complete tumor resection (Aibar-Durán et al., 2020).

1.4. Functional reorganization

1.4.1. History

The term *plasticity* was first used by William James in 1890 in his book *The Principles of Psychology*, a treatise on behaviorism (James, 1890). The word itself is based on the ancient Greek word *plastikos*, meaning “formable”. This word describes structural alterations of the brain in response to environmental changes.

One century ago, the Italian surgeon Vincenzo Malacarne had already formulated the hypothesis of the cerebellum being plastic and growing according to its tasks. He developed this idea during his postmortal dissection studies when he had counted many more cerebellar lamellae in intellectual individuals than in uneducated ones (Zanatta et al., 2018). Later, different scientists adopted this line of thought. Charles Darwin was among those scientists. He noticed that domestic rabbits had smaller brains than their wild counterparts, which he traced back to their confined environment (Darwin, 1874).

Since it was already commonly accepted that the brain must undergo a change in some manner to enable memory, psychologist Donald Hebb proposed his theory in 1949. According

to Hebb, one nerve cell that repeatedly excites another nerve cell leads to synaptic strengthening and, ultimately, learning. Today, this theory is called “Hebb’s rule” and is concisely summarized as “What fires together, wires together” (Hebb, 1949).

In the 1900s, an American research group from the University of California, Berkeley, became pioneers in this field by conducting animal experiments to produce scientific evidence for plastic changes in the central nervous system. They discovered that rats living in a challenging and stimulating environment developed thicker cortices and showed increased neuronal enzymatic activity. These changes did not depend on age. Instead, these changes occurred equally in young and old specimens (Bennett et al., 1996).

Today, instead of using the word *plasticity*, the term *functional reorganization (FR)* is commonly used, as it describes the development processes activated by environmental changes better and is exclusively neuroscientifically related.

1.4.2. Modern concept

1.4.2.1. Overview

Functional reorganization is a perpetual process. It allows the brain to adjust continually to a changing environment by optimizing its neuronal networks beyond the restrictions of its own genome (Pascual-Leone et al., 2005). It enables people to memorize information and learn new skills. Synaptic changes are done so cleverly that simultaneously, thinking processes become accelerated, and energy needs decrease.

Altering a working system also has destabilizing effects. Hence, the question arose about how complex neuronal circuits “survived” FR. Upon closer examination, regulating mechanisms were found, which constantly prevent the system from collapsing. Thus, the concept of a *homeostatic* FR was born (Turrigiano and Nelson, 2004).

Taking one step back there is another level of brain plasticity. A consistent stimulus does not lead to uniform effects in comparable neurons. Rather, the efficacy of synaptic transmission depends on the single neuron’s history of activity, which triggers either a long-term depression (LTD) or long-term potentiation (LTP). This higher-order form of neuroplasticity is called *metaplasticity* (Abraham and Bear, 1996).

1.4.2.2. Levels

Functional reorganization takes place both microscopically and macroscopically. On the microscopic level, neurons are constantly converting through the proliferation of dendritic branches, growth of axons, strengthening of old synapses, and formation of new synapses. At the same time, homeostatic mechanisms prevent unfocused chaos of neuronal wiring by inducing apoptotic processes. In this manner, circuits are refined, outliers are eliminated, and electric signals are thus pooled. These microscopic alternations are so substantial that the

macroscopic structure of the brain also continually changes. Similar to training a muscle, frequently challenged cortical areas grow over time.

In addition to macroscopic and microscopic, FR can be subclassified as structural and functional. Structural FR includes all the anatomically and histologically observable changes, whereas the varying efficacy of synaptic transmission is called functional FR (Duffau, 2006).

1.4.2.3. Principles

Functional reorganization does not happen randomly or on its own. Instead, it needs some sort of stimulus to influence the quality, speed, and direction of functional reorganization. Fundamentally, FR occurs in three different ways: via training, lesion-triggering, or maladaptation.

A TMS study on blind readers of Braille has shown an expansion of the cortical sensorimotor representation of their reading finger (Pascual-Leone and Torres, 1993). Another study found an increased cortical representation of the left-hand fingers of stringed instrument players via magnetic source imaging (Elbert et al., 1995). These studies prove that training specific muscles lead to a greater cortical representation of these body parts. This also works in reverse. Immobilization of body parts causes shrinkage of the related functional areas on the precentral cortex (Liepert et al., 1995). There have been similar findings concerning somatosensory, visual, and auditory cortices. For instance, blind people have a relatively enlarged cortical area responsible for auditory discrimination of frequencies compared to sighted humans. Furthermore, they seem to process auditory and tactile information in the visual cortex, which would otherwise remain unused (Elbert and Rockstroh, 2004).

There are two kinds of lesions leading to plastic cortical changes: intra- and extracerebral lesions. Intracerebral lesions, such as strokes, bleedings, or tumors directly destroy functional areas, whereupon FR activates to preserve skills. The more slowly the destruction takes place, the more time there is for plastic adaptation and compensation of deficits. For this reason, slow-growing gliomas can become considerably large before any impairment occurs (Szalisznyo et al., 2013). Concerning extracerebral lesions, a sudden lack of afferent information due to amputation or nerve injury leads to significant and abrupt cortical reorganization. Intact adjacent cortical regions “invade” the newly unemployed area (Pons et al., 1991).

Such deafferentations can lead to maladaptive reorganization, resulting in symptoms such as phantom limb pain or tinnitus (Elbert and Rockstroh, 2004; Flor et al., 1995; Mühlnickel et al., 1998).

1.5. Objectives

By studying glioma patients who underwent awake craniotomy and DES for at least two times, researchers have detected cortical FR (Southwell et al., 2016). As a research team focusing on nTMS diagnostics, we wondered if this tool was also able to measure FR. Compared to DES, nrTMS language mapping shows an especially high correlation concerning language-negative sites (LNS) (Krieg et al., 2014a; Picht et al., 2013). Consequently, we wanted to analyze changes in LNS in glioma patients over time on potential dynamics (Ille et al., 2019).
It is known that injuries to cortical areas can impair language function and that minimal damage to subcortical pathways can cause major impairments. Thus, a better understanding and visualization of language networks are crucial in the field of neurosurgery. We planned on using language positive sites (LPS) as determined by nrTMS performed on glioma patients as a starting point for performing FT. These sites would also be used to correlate quantitative changes in subcortical fibers with language function (Ille et al., 2018).

2. MATERIALS AND METHODS

2.1. Ethics

The experimental setup for both studies was approved by our local ethics committee (registration number: 222/14) and was conducted in accordance with the Declaration of Helsinki. Written informed consent was obtained from all patients prior to the examination (Ille et al., 2019; Ille et al., 2018).
Furthermore, we were always adhering to the “safety, ethical considerations, and application guidelines for the use of transcranial magnetic stimulation in clinical practice and research” by Rossi et al. (Rossi et al., 2009).

2.2. Patients

Eighteen patients (13 males and five females) suffering from left-sided brain lesions affecting language were treated consecutively in the Department for Neurosurgery at the Klinikum rechts der Isar MRI TUM between 2012 and 2018. All patients underwent at least two tumor resections, and preoperative nrTMS language mapping was performed each time.
Minors under the age of 18 years and patients who met the general TMS exclusion criteria (contraindications: cochlear implant, internal pulse generator, medication pumps) were excluded (Krieg et al., 2017; Rossi et al., 2009; Rossini et al., 2015). Additionally, patients suffering from advanced-stage aphasia, which made nrTMS language mapping impossible, were not included. (Ille et al., 2018).

2.3. Navigated repetitive transcranial magnetic stimulation (nrTMS)

2.3.1. Concept

nrTMS language mapping creates a short-term, transient cortical lesion using magnetic stimulation. The patient is instructed to perform a time-locked object naming task. In the meantime, a disturbance to performing the task occurs if areas are stimulated that are not necessary to perform the task.

2.3.1.1.Fundamental technique

The basic principle of TMS is to place a wire coil tangentially on the patient's head, just above the cortical target area. As soon as power is applied, a strong magnetic field forms that induces an electrical field within the cortex, which in turn stimulates neurons by depolarization (Barker et al., 1985).

Concerning the coil, there are different designs to choose from depending on the target area depth. Studies have proven that a figure-of-eight coil is the most effective type for cortical region stimulation. This shape takes advantage of the following physical effect: Once the electrical circuit is closed, current flows through both circles, and each circle produces its own magnetic field. As the circles touch under the center of the coil, their two fields combine, doubling their power. In this way, a highly concentrated magnetic field is created, which in turn induces a focally limited intraparenchymal electric field. Making use of this effect on point stimulations is possible (Deng et al., 2013; Ueno et al., 1988). Stimulations are conducted by bipolar pulses, causing transient changes to membrane potential, which in turn trigger action potentials. The volume of the activated tissue depends on the pulse's intensity. A larger area becomes activated as the intensity is increased. As activation of smaller volumes results in more precise mapping, the intensity of stimulation is chosen slightly above the individual threshold of activation (Krieg, 2017).

2.3.1.2. nrTMS language mapping

Mapping language function differs from mapping motor function. When mapping language function, no positive vocal reaction can be caused by single-pulse stimulation. Thus, the technique is used in reverse. The test person is obliged to talk throughout the entire examination while being stimulated with repetitive pulses. An abrupt disruption in performance occurs if a transient cortical lesion occurs within language eloquent areas. Experience from many years of DES application has demonstrated that object naming is the most suitable task for evaluating language performance (Petrovich Brennan et al., 2007). Synchronized videotaping of the whole session and subsequent analysis can be used to further improve the quality of the results (Lioumis et al., 2012). The information gained regarding LPS and LNS is uploaded into the neuronavigational system via the DICOM (Digital Imaging and

Communications in Medicine) Standard. This process assists the neurosurgeon not only in planning the procedure but also perioperatively by displaying the information on the screen.
Even today, there is no superior method than DES during awake craniotomy for mapping language function. Thus, it is generally acknowledged as the gold standard. DES results also serve as a benchmark for other non-invasive mapping techniques. In direct comparison to DES, it has been repeatedly proven that TMS has an especially high sensitivity and negative predictive value concerning the mapping of LNS. This negative mapping is of great importance in preoperative assessment, as it identifies resectable cortical areas (Krieg et al., 2014a; Picht et al., 2013).

2.3.2. Tools

2.3.2.1.Software

A crucial requirement for this examination is a solid navigation in three-dimensional space, enabling the performance of a precise point-by-point stimulation. Concerning software and hardware, we used the eXimia nTMS system version 4.3 and a compatible NexSpeech module, both designed by the Finnish company Nexstim (Nexstim Plc, Helsinki, Finland).
The NexSpeech software creates a three-dimensional (3D) head model using MRI imaging. It enables the examiner to prepare the session, set marks, determine stimulation sites, and most importantly, perform a precise and controlled mapping.
Concerning the fed-in imaging, T1-weighted 3D MRI scans with 1 x 1 x 1 mm voxel size were used. All patients received MRI scans by default: a preoperative one for planning the surgery and a postoperative one to assess the extent of resection (EOR) and exclude any hemorrhage or ischemia. MRI scans were enhanced by intravenous contrast media and included a three-dimensional gradient-echo sequence and diffusion tensor imaging (DTI) with 32 orthogonal sequences. For the present study, the MRI scanner Achieva 3T was used (Philips Medical System, Netherlands B.V.) (Ille et al., 2019). The resulting data set was uploaded via DICOM Standard into the NexSpeech software.

2.3.2.2. Hardware

Another aspect of this examination technique is the necessity to merge the shape of the actual patient's head with the virtual model and then perceive the examination tools in a spatial relationship. Through a stereotactic approach, this complex task is accomplished in real time. The patient themselves, in addition to the required tools (e.g., coil and digitizer pen), are equipped with several reflectors, which are recognized by an infrared camera installed in front of the patient. In the past, patients wore goggles or a headband bearing these reflectors. However, these constructions bore the risk of inadvertent movement during the session. Currently, a disposable head tracking device is stuck on the patient's forehead, allowing for free head movement while ensuring a maximum accuracy.

For the software to align the patient's head with the virtual MRI head model, the examiner follows a software-guided registration process. During this process, a digitizer pen is pointed at three predefined MRI landmarks—the nasion and the crus of the helix in each ear—and nine set circles around the head. Eventually, the head as a whole is linked to the MRI model within 2 mm accuracy (Krieg, 2017).

The stimulation device is a current-carrying figure-of-eight coil that develops a magnetic field strength of 2.2 Tesla. To ensure a maximum accuracy, the examiner must pay special attention to the right coil orientation and inclination during the mapping procedure.

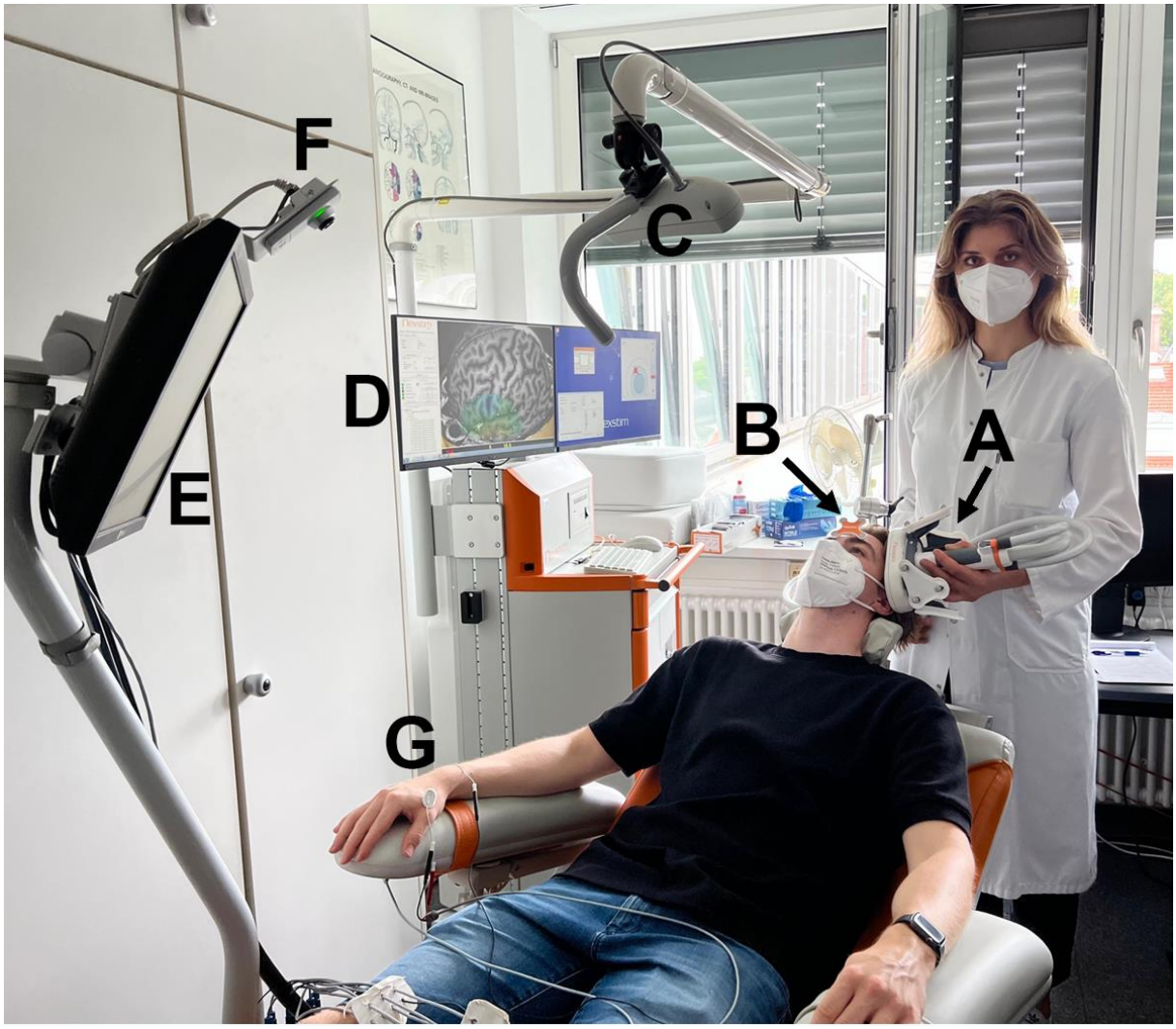

Figure 3 *Experimental setup of an nrTMS language mapping device*

Used system is the eXimia system by Nexstim (Nexstim Plc, Helsinki, Finland). The patient wears a head tracking device (B) that is stimulated with a coil (A) guided by the examiner. Both A and B are equipped with reflectors, which are perceived by a stereotactic camera (C). The spatial data are integrated into the neuronavigational application—NexSpeech, by Nexstim (Nexstim Plc, Helsinki, Finland), which is displayed on a double screen (D). Patients are presented with the object naming task on an adjustable screen in front of them (E). A video

camera sets just above that screen (F), and it records the patient's performance for the subsequent analysis. An electromyography is conducted from electrodes (G) attached to small hand muscles of the dominant hand to initially determine the resting motor threshold (rMT). Stimulation pulses are released by stepping on a pedal.

2.3.3. Preparation

An examination of the patient's neurological status was performed at least six times, as the two surgeries were each accompanied by three examinations:

- 1st surgery: Preoperatively (PRE-1), five days postoperatively (POD5-1), and three months postoperatively (POM3-1).
- 2nd surgery: Preoperatively (PRE-2), five days postoperatively (POD5-2), and three months postoperatively (POM3-2)

(Ille et al., 2019)

In every examination, we recorded each patient's history of seizures, severity of aphasia, and handedness.

Handedness was determined via the Edinburgh Handedness Inventory (EHI), which provides a laterality quotient (LQ) between −100 and +100 (Oldfield, 1971). We defined a right-hander as having an LQ above +40, a both-hander as having an LQ between +40 and −40, and a left-hander as having an LQ below −40. Of the 18 included patients, 15 were right-handed, two were both-handed, and one was left-handed.

In order to assess language function, we used a modification of the Aachen Aphasia Test (AAT), a German speech-impairment grading (Huber et al., 1980).

Aphasia:

0 no impairment of language function
1 slight impairment of daily communication
2 moderate impairment of language function, communication possible
3 severe impairment of language function, no communication possible

Dominating impairment:

A predominantly motor impairment non-fluent speech
B predominantly sensory impairment fluent speech

Afterward, the patient was issued a 13-item safety questionnaire to minimize any risks potentially associated with the TMS technique. The questionnaire requires the patient to list any history of neurological diseases, such as seizures, concussions, or syncopes; hearing

problems; pregnancy; current medication; or implanted metal devices (general TMS exclusion criteria) (Krieg, 2017).
Finally, the whole procedure was explained to the patient, and if no further questions were asked, the examination was executed.

2.3.4. Workflow

We performed nrTMS language mappings on patients according to our standard protocol (Krieg et al., 2017). First, the MRI scan was fed into the nTMS system to reconstruct a 3D head model. This model was displayed on the screen during the whole session, enabling the examiner to navigate the coil precisely.
Since an average language mapping lasted at least one hour, providing the patient with maximum comfort while seating them at the beginning was a crucial way to improve compliance and concentration throughout the whole session. Once the head trackers were fastened, the registration process was carried out, as previously described.
First, the patient's best individual stimulation intensity was determined via a scaled-down motor mapping. The lowest possible mapping intensity that would still result in a sufficient motoric reaction was identified. This lowest intensity is the so-called resting motor threshold (rMT). Previous studies have shown that using this same value in the consecutive language mapping produces the best results. An electromyography (EMG) electrode was adhered to the target muscle (usually the abductor pollicis brevis) and one earth electrode was stuck on a nearby bony prominence to track motor-evoked potentials (MEPs). As EMG signals are extremely sensitive and easily disrupted by poorly positioned electrodes or insufficiently relaxed muscles, the quality of the EMG derivative was thoroughly checked on the screen before performing any stimulation.
The precentral gyrus, starting with the hand knob, was roughly mapped with the standard intensity of 80–100 V/m.
While keeping an eye on the EMG, the stimulation was aimed at the area that produced the most uniform and repeatable contraction of the target muscle. In this way, its connected cortical hotspot was identified. This spot was then saved and used to determine the rMT with the least intensity while still producing an excitation of the motor cortex followed by a clear muscular response. This response needed a peak-to-peak amplitude of no less than 50 µV (Krieg et al., 2017; Krieg et al., 2012).

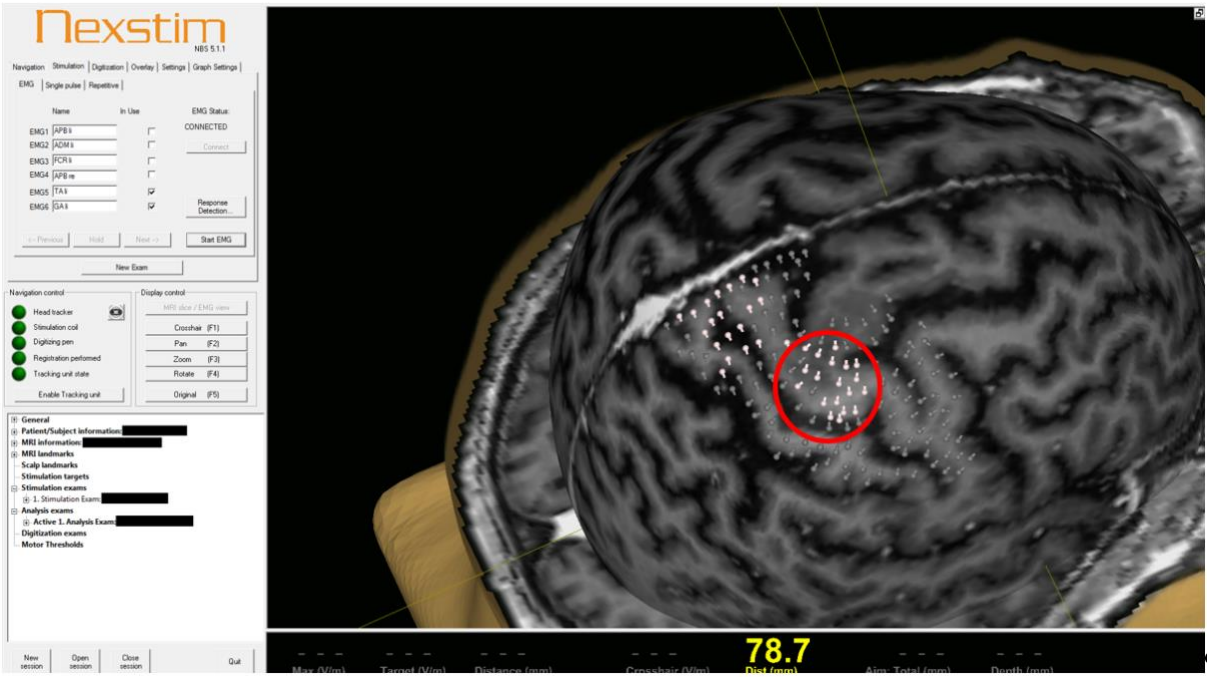

Figure 4 *View of the working screen during the hotspot identification*
As this is a left-handed patient, the right hemisphere is turned up front to map the right sided precentral gyrus. Electromyography (EMG) electrodes on specific hand-muscles conduct the muscular response. The EMG is displayed on a second screen. The location of every performed stimulation is marked by a pin. White colored pins indicate a positive, grey pins a negative muscular response. The hotspot identification is always started at the handknob (circled in red). This round, cortical area of the precentral gyrus contains most likely the pyramidal cells activating the hand muscles, just as in this case.

As the last preparatory step, a baseline examination was performed. The patient was confronted with the object naming task (consisting of 131 different black and white images) without stimulation but with the same picture displaying timeframes as with stimulation. Unfamiliar objects, or those that the patient had difficulty naming, were excluded. This task was repeated twice until all the critical images were ruled out. If the patient was unable to name more than 60% of the images correctly, we excluded him due to severity of aphasia (Ille et al., 2018). The picture order was changed at random with every display to avoid habituation. Since the baseline was filmed and saved just like the actual mapping, the patient's performance acted as a benchmark for comparing his performance under stimulation conditions later on.
After all preparations were completed, the actual mapping was performed under the following standard parameters:

- Intensity = 100% of the rMT
- 1 stimulation = 5 pulses within 1 sec
- Picture-to-trigger interval = 0 ms

- Display time (time one picture is shown) = 700 ms
- Interval time (time between two pictures) = 2,500 ms

In 2015, a system for nrTMS language mapping had been established, consisting of 46 anatomically defined points spread over the whole hemisphere (Hauck et al., 2015). Underlying the points' allocation served the cortical parcellation system (CPS), a pattern for subdividing the cortex into anatomical parts (Corina et al., 2005). Areas above parts of the frontal and temporal lobes were not included in the 46 spots, as stimulation of these regions is known to cause intolerable pain for the patient (Krieg et al., 2013). Additionally, the whole gyrus temporalis inferior was excluded from the system. The distance between skin and brain is too far due to the marginal anatomic location of this gyrus, making a sufficient stimulation impossible (Krieg et al., 2013).

In order to prepare for a language mapping session, the examiner identified and tagged each of the 46 points on the 3D MRI head model in advance. During the mapping itself, the coil was simply aimed at these marks. Simultaneously, the patient had to carry out the object naming task, which they had already become familiar with. With every image shown, one stimulation was emitted. Every cortical spot was stimulated three times per round. In total, two rounds per hemisphere were conducted, totaling 552 stimulations.

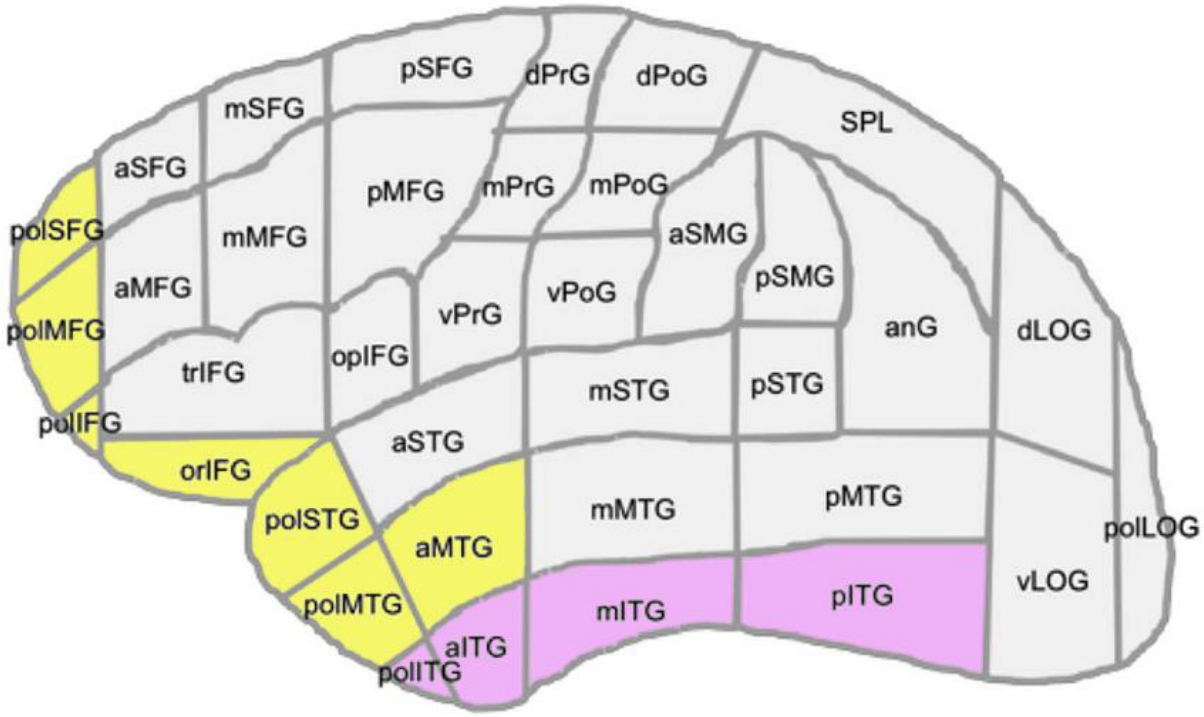

Figure 5 *Cortical parcellation system*

As introduced by Corina et al. in 2005 (Corina et al., 2005). Colors represent areas that were excluded from stimulation: yellow areas were not stimulated because of known painfulness, and pink areas were not stimulated because of inaccessibility.

Abbreviation	Anatomy
aITG	Anterior inferior temporal gyrus
aMFG	Anterior middle frontal gyrus
aMTG	Anterior middle temporal gyrus
anG	Angular gyrus
aSFG	Anterior superior frontal gyrus
aSMG	Anterior supramarginal gyrus
aSTG	Anterior superior temporal gyrus
dLOG	Dorsal lateral occipital gyrus
dPoG	Dorsal post-central gyrus
dPrG	Dorsal pre-central gyrus
mITG	Middle inferior temporal gyrus
mMFG	Middle middle frontal gyrus
mMTG	Middle middle temporal gyrus
mPoG	Middle post-central gyrus
mPrG	Middle pre-central gyrus
mSFG	Middle superior frontal gyrus
mSTG	Middle superior temporal gyrus
opIFG	Opercular inferior frontal gyrus
orIFG	Orbital part of the inferior frontal gyrus
pITG	Posterior inferior temporal gyrus
pMFG	Posterior middle frontal gyrus
pMTG	Posterior middle temporal gyrus
polIFG	Polar inferior frontal gyrus
polITG	Polar inferior temporal gyrus
polLOG	Polar lateral occipital gyrus
polMFG	Polar middle frontal gyrus
polMTG	Polar middle temporal gyrus
polSFG	Polar superior frontal gyrus
polSTG	Polar superior temporal gyrus
pSFG	Posterior superior frontal gyrus
pSMG	Posterior supramarginal gyrus
pSTG	Posterior superior temporal gyrus
SPL	Superior parietal lobe
trIFG	Triangular inferior frontal gyrus
vLOG	Ventral lateral occipital gyrus
vPoG	Ventral post-central gyrus
vPrG	Ventral pre-central gyrus

Anatomical names and abbreviations are according to Corina et al. 2005.
doi:10.1371/journal.pone.0075403.t003

Table 1 *Abbreviations contained in the cortical parcellation system (Corina et al., 2005); Image (Krieg et al., 2013)*

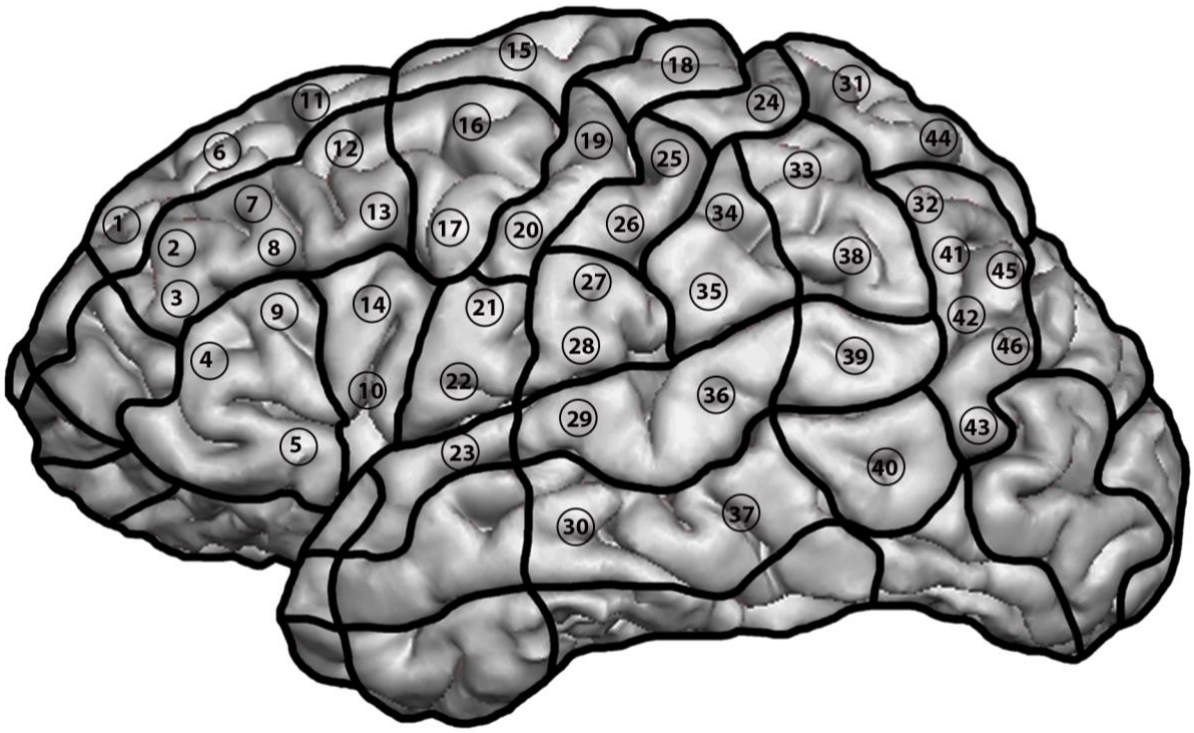

Figure 6 *46 language stimulation sites distributed on the cortical parcellation system (Corina et al., 2005)*

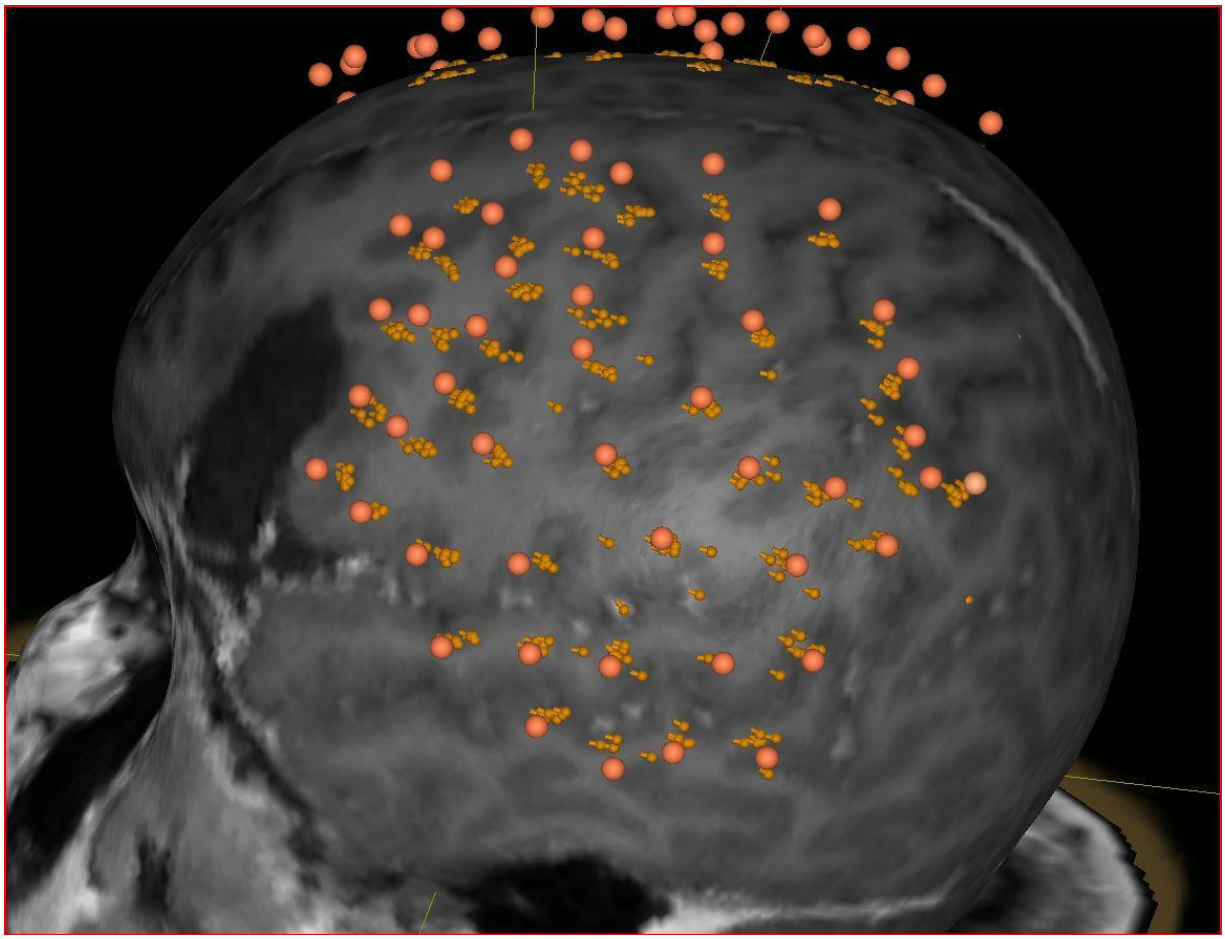

Figure 7 *Exemplary excerpt of a completed language mapping session*
Underlying is the three-dimensional head model, where the left hemisphere is turned front. The large orange dots mark the 46 language stimulation sites, which were positioned in advance according to anatomical aspects. The smaller, lighter-colored pins mark each real stimulation spot. Even though the examiner aims for six stimulations per mark, outliers do occur (see image). They are dealt with individually in the analysis later on.

2.3.5. Analyzing responses

Once the examination was finished, the raw data was uploaded into the NexSpeech analyzer software. The working screen displayed the session's video recordings next to the baseline performance. The images of the object naming task appeared time-locked on the bottom of the screen. In this way, the examiner was able to re-experience the whole session and search for sudden decreases in performance, such as inconsistencies in pronunciation or delays in responses. When a potential error was detected, the section was compared to the baseline performance. Errors were classified within four different categories:

- **No response:** complete lack of verbal response or delay of more than 1 sec (after the fifth pulse). This is the most reliable kind of error (Krieg et al., 2016; Sollmann et al., 2014).

- **Performance:** anomalies in pronunciation, such as stuttering, babbling, or different accentuation.
- **Semantic:** confusion of the correct expression with something related (e.g., “hand” instead of “foot”).
- **Other:**
    - Neologism (creation of a new word)
    - Phonological errors, such as clipping syllables (e.g., *“Nana” instead of “Banana*”) or the mission of consonants (*e.g., ”Pape” instead of “Paper”*).
    - Circumlocution (describing the meaning without using the actual term).

When finished, an analysis report was automatically created, containing each type of error, clarity, image name, NBS nrTMS sequence ID, and comments.
The collected data were fed into the neuronavigation system and forwarded to the surgeon for planning and performing the procedure.
In this study, we decided to discard errors due to hesitation (delay of response, starting between the fourth and fifth pulses), as these errors were repeatedly classified as being untrustworthy by previous authors (Lioumis et al., 2012). Clearly, errors resulting from pain or direct muscle stimulation were also excluded.

2.4. Fiber tracking

2.4.1. Data composition

We performed FTs on three different occasions. Ten patients could be included (IDs: 3, 5, 9, 11, 12, 13, 14, 16, 17, and 18). We worked with the FT software iPlanNet Cranial 3.0.1 (Brainlab AG, Munich, Germany), using our standard deterministic algorithm with a fiber assignment by continuous tracking (FACT) (Ille et al., 2018).
For each patient, the raw data consisted of the results of two nrTMS language mappings plus MRI scans at three different points in time. As illustrated in Figure 10, each FT comprised one nrTMS mapping and its affiliated MRI scan. The PRE-1 nrTMS mapping data were used twice.

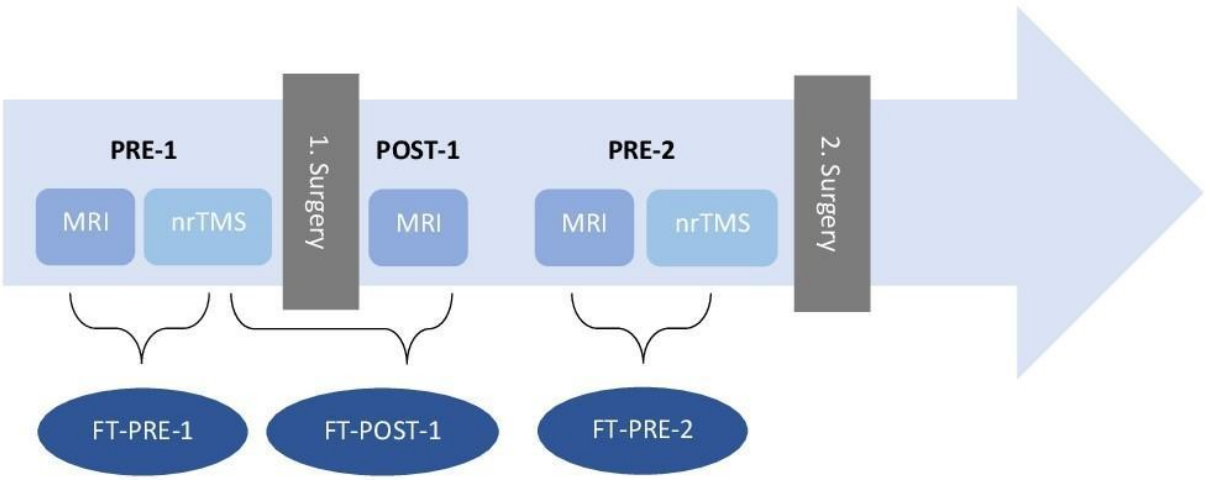

Figure 8 *Data underlying each fiber tracking*

- *Fiber tracking at PRE-1 (before 1st surgery): PRE-1 MRI + PRE-1 nrTMS*
- *Fiber tracking at POST-1 (after 1st surgery): POST-1 MRI + PRE-1 nrTMS*
- *Fiber tracking at PRE-2 (before 2nd surgery): PRE-2 MRI + PRE-2 nrTMS*

Concerning the MRI scans, two different sequences were required: A DTI study and a 3D MP-RAGE. Once uploaded into the FT software, these image stacks were fused together along their anatomical landmarks and transformed into a 3D object.

2.4.2. ROI seeding

Before FTs could be performed, the software required defined cortical starting points, the so-called ROIs. We chose two different approaches for ROI seeding. First, we wanted to perform an entire language network tractography. Therefore, we used all the left-sided LPS as determined by the nrTMS language mapping completed beforehand, plus a rim of 5 mm each. Furthermore, we defined additional subcortical ROIs for FTs of three major white-matter pathways (WMPs), contributing to the *dual stream model of language*.

- IFOF: ROI within dorso-rostrally oriented fibers of the external capsule.
- FAT: ROI within cranio-caudally oriented fibers, connecting the superior frontal gyrus to the inferior frontal gyrus.
- SLF/AF: ROI within dorso-rostrally oriented fibers located laterally to the posterior horn of the lateral ventricle.

(Ille et al., 2018)

2.4.3. Analysis

To refine and modulate results, we set limits for a minimum fiber length (MFL) and anisotropy. The degree of anisotropy is called fractional anisotropy (FA) (isotropic = 0, anisotropic = 1). The aim was to set these parameters in such a way that the resulting bundles would contain

as many fibers as possible while having a minimum number of outliers at the same time. For every patient, we used the same parameter combinations recently published as optimal settings: (FA-MFL) 0.10–100, 0.15–100, 0.15–90, 0.15–80, and 0.20–70 (Negwer et al., 2017b).

We added one more setting, which proved reasonable in clinical practice, to these five settings: 0.20–100.

Finally, we counted the total number of fibers and the fibers of each WMP. To assess decreases or increases in the number of fibers, we calculated percentage changes between PRE-1 and POST-1, POST-1 and PRE-2, and PRE-1 and PRE-2 (Ille et al., 2018).

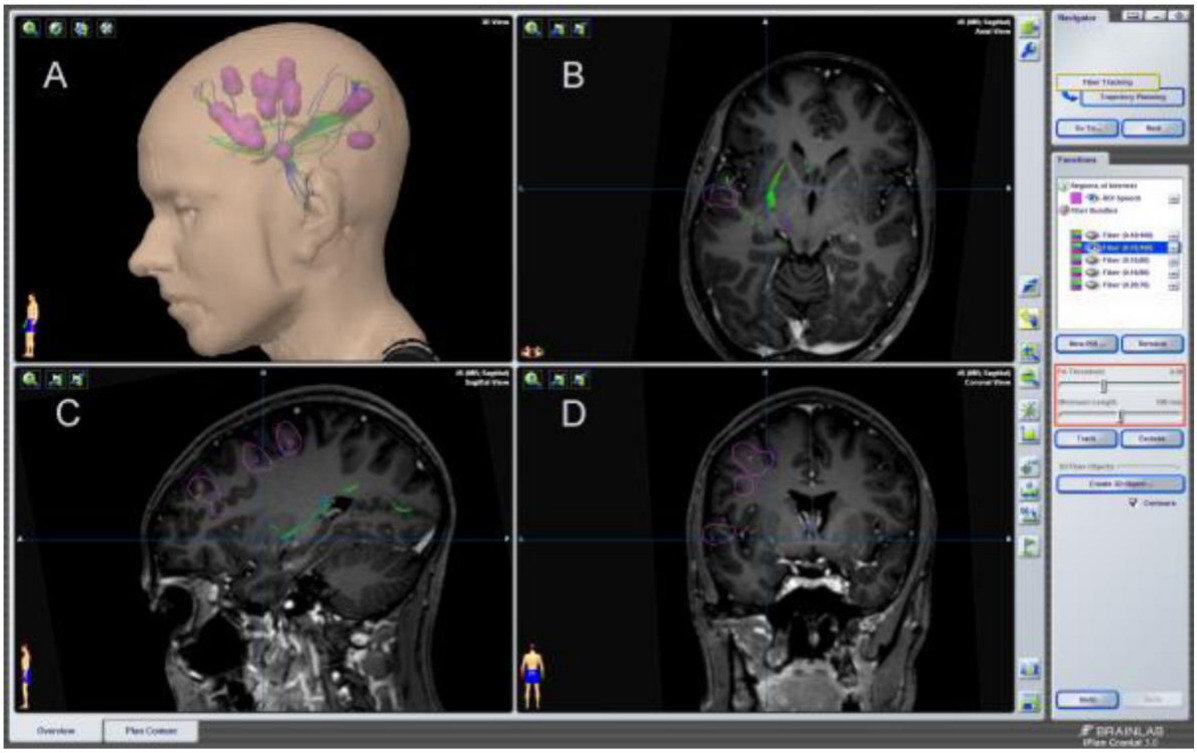

Figure 9 *Control panel of the tractography software*

A: 3D reconstruction of the navigational MRI with the ROIs (pink) and reconstructed color encoded fibers. B: axial MRI sequence. C: sagittal MRI sequence. D: coronal MRI sequence. Red rectangular frame: rulers to define MFL and FA threshold.

(Negwer, 2018). *Image used with permission from PD Dr. med. Chiara Negwer.*

2.5. Surgery

There are two competing goals regarding operating on language eloquent brain lesions. While surgeons strive to achieve the most radical EOR possible, this goal is overshadowed by the aim of preserving language function and, therefore, quality of life. The gold standard in detecting language eloquent areas is DES during awake craniotomy (De Witt Hamer et al., 2012; Sanai et al., 2008).

To ensure a patient is eligible for the procedure, sufficient language function and mental fitness are crucial (Milian et al., 2014; Picht et al., 2013). If the patient fails the requirements, DES is no longer an option. Instead, a fully asleep approach to surgery is chosen.

Concerning the course of surgery, we were compliant with the guidelines for awake craniotomies at all times (Picht et al., 2006; Talacchi et al., 2013).

Significant parts of the surgery (i.e., craniotomy, resection of parts distant from function, and skull closure) were performed under total intravenous anesthesia (TIVA). Intraoperatively, the patient was temporarily woken up to undergo the DES. For this part, a trained neuropsychologist was in charge of leading the same object naming task as in the preoperative nrTMS mapping. The trained neuropsychologist was also in charge of evaluating language performance. The presence of a neuropsychologist was crucial, as it supports shorter durations of surgery and higher rates of gross total resection (Kelm et al., 2017). In the meantime, the surgeon was stimulating the exposed cortical tissue bit by bit to identify eloquent areas. The tools used were a bipolar electrode for cortical areas and a monopolar electrode for subcortical white matter. Once the mapping was completed, the surgeon started to resect the tumor microsurgically. All the while, language function was monitored via continuous overt speech.

As precise orientation is crucial for brain surgery, a neuronavigational system (Brainlab Curve, Brainlab AG, Munich, Germany) was used by default, and surgeries were performed in a stereotactic manner. The system combined the preoperative fMRI with the anatomical MP-RAGE data set, the preoperative nrTMS language mapping results and the DTI FTs. These data were fused together and displayed on the screen during surgery. Similar to nrTMS mappings, intraoperative stimulation sites were located in the digital head model, as all the key devices (i.e., Mayfield clamp, stimulation electrodes, and navigation pointer) were equipped with reflectors that were detected by an infrared camera.

2.6. Analysis

2.6.1. Division of the cortex

The majority of cortical language eloquent areas is located in perisylvian parts of the cortex. Therefore, we focused on analyzing these regions. In general, anterior areas are known to be responsible for speech production, whereas posterior areas cover speech perception and comprehension. To account for this partitioning in our analysis, we split up the perisylvic-located CPS areas into anterior and posterior ones.

In the anterior portion, we enclosed the three CPS areas—triangular inferior frontal gyrus (trIFG), opercular inferior frontal gyrus (opIFG), and ventral pre-central gyrus (vPrG)— which contain seven standard language stimulation sites (4, 5, 9, 10, 14, 21, and 22).

The posterior part consisted of the five different CPS areas—angular gyrus (anG), anterior supramarginal gyrus (aSMG), posterior supramarginal gyrus (pSMG), middle superior temporal gyrus (mSTG) and posterior superior temporal gyrus (pSTG)—which contain 13 language stimulation sites (29, 32, 33, 34, 35, 36, 38, 39, 41, 42, 43, 45, and 46).
In addition to this uniform separation, we defined a tumor area (TA) and an area without tumor (WOT) for each patient. The areas we defined corresponded to their preoperative MRI scans. In this way, we subdivided our patients into two groups: one with anterior (A) and one with posterior (P) tumors (Ille et al., 2015a).

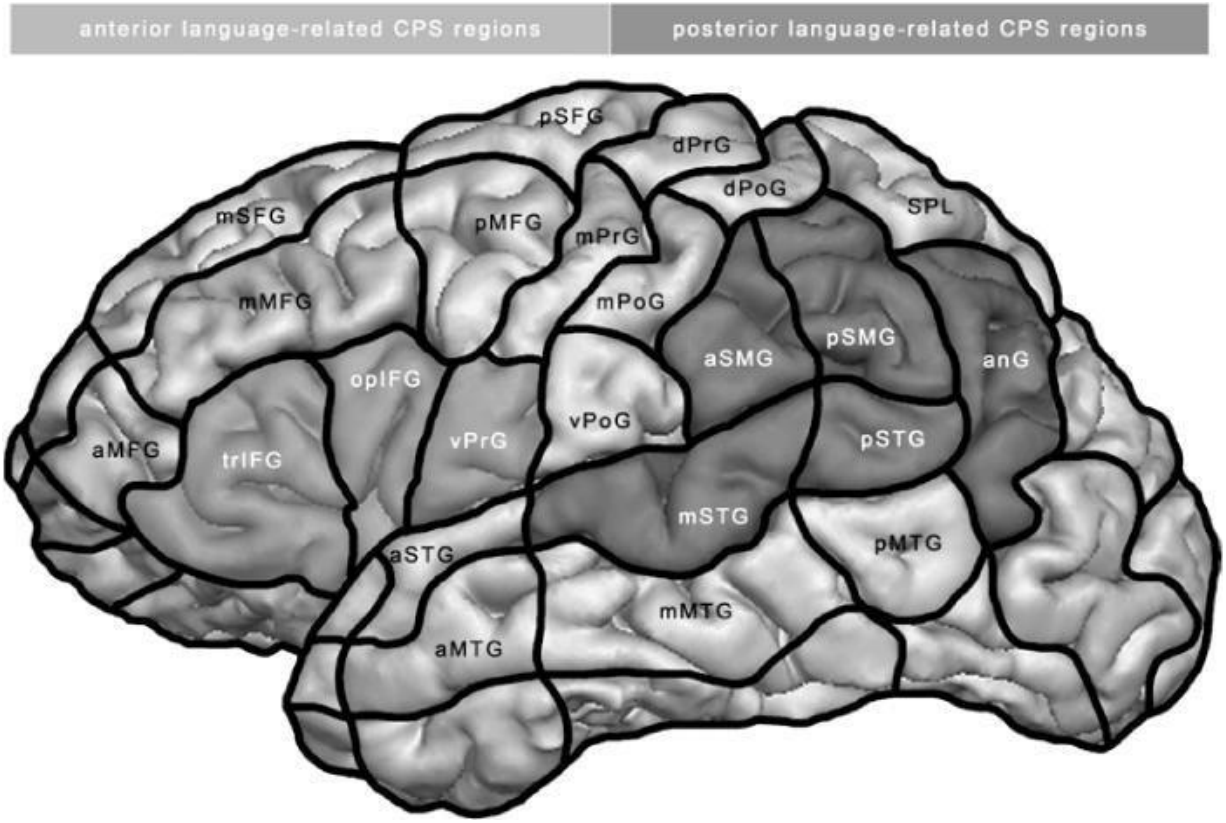

Figure 10 *Subdivision of the perisylvian cortex*
The perisylvian cortex is subdivided into anterior (light grey) and posterior (dark grey) language-related region, based on the cortical parcellation system, as introduced by Corina et al. (Corina et al., 2005).
(Ille et al., 2015a)

2.6.2. Data organization with regard to functional reorganization

2.6.2.1. nrTMS data

Thus far, we have been focusing on LPS in terms of nrTMS data collection. An LPS is defined as a stimulation site that shows at least one valid error during nrTMS mapping. However, research has repeatedly confirmed that compared to the gold-standard technique of DES, nrTMS especially stands out for its high sensitivity and negative predictive value (NPV) (Ille et

al., 2015a; Krieg et al., 2014b; Picht et al., 2013; Tarapore et al., 2013). A high NPV means that stimulation sites that tested negative have a high probability of truly being negative. Therefore, the analysis of LNS is especially significant. Language negative sites are defined as “all other stimulation sites that are not classified as LPS.”

Thus, we based our analysis targeting FR on LNS, as it is more reliable than LPS.

We compared the changes of left-hemispheric LNS in the TA and WOT for every patient.

Afterward, we combined the LNS of all included patients and calculated means depending on the following characteristics:

- Language near tumor
- Aphasia after first surgery (in POD5-1)
- Surgery-related deficit
- Tumor-related deficit
- Seizures

We calculated *p*-values for evaluating the dependence of LNS on these characteristics to expose their impact on FR.

Consequently, we implemented a case-by-case study in a variety of different categories and correlated the nrTMS data with this additional information. We decided to incorporate the following characteristics:

- WHO grade
- Time between mappings
- Language deficits
- Tumor location
- Interhemispheric dominance ratio (HDR) and intrahemispheric dominance ratio (IDR)
- Predominant location of language function
- Seizures
- Handedness
- Anti-epileptic drugs (AED)

(Ille et al., 2019)

2.6.2.2. Fiber tracking data

Concerning FTs we used the opposite raw data, than in the study on cortical FR. For the execution of FTs there was no other option than using LPS as starting points for tracing pathways. Once we ran the tracking, we calculated the number of fibers for each of the three FTs (PRE-1, POST-1, and PRE-2) for the whole language network and for the three WMPs separately.

We were especially interested in patient parameters that caused a diminution of fiber numbers (e.g., postoperative subcortical ischemia), or were a symptom of a decrease of fiber numbers (worsening of aphasia).
Furthermore, we pooled patients into the following groups, depending on the occurrence of new language impairments:

- Permanent surgery-related language deficit (impairment first occurred at POST-1 and is still persistent at PRE-2)
- Transient surgery-related language deficit (impairment did first occur at POST-1 and disappeared by PRE-2).
- New tumor-related language deficit (no language deficit at POM3-1, new language deficit at PRE-2 plus tumor recurrence in MRI scan)
- No new language deficit

(Ille et al., 2018)

2.6.3. Statistical analysis

2.6.3.1. ER analysis

To handle the nrTMS data beyond the information given by the automatically created session report, we set up an Excel table (Microsoft Excel, Microsoft Corporation, Redmond, Washington, USA) connecting each error and its type to its stimulated spot in both subdivision systems (46 language sites, CPS). Additionally, the number of trials per spot was entered.
From this data, error rates (ER) were calculated. ERs are defined as "the number of errors per number of trials" and were always represented by a number between 0 and 1 (Krieg et al., 2013; Picht et al., 2013). An ER was calculated for every stimulated spot, including posterior (pER) and anterior (aER) language areas. An ER was also calculated for each hemisphere. We used these hemispheric ERs to calculate the HDR (HDR = ER left hemisphere divided by ER right hemisphere; HDR > 1 left-dominant, HDR < 1 right-dominant). In the same manner, we calculated an HDR in the contralateral anterior language areas (aHDR) and the contralateral posterior language areas (pHDR). Within each hemisphere, we determined an IHR by dividing the aER by the ipsilateral pER (Ille et al., 2019).

2.6.3.2. LNS analysis

We used inferential statistics in an attempt to apply conclusions drawn from individual patients to the whole population. We anticipated the detection of LNS shifts by comparing the two nrTMS mappings. Furthermore, we strived to correlate potential changes with additional patient characteristics.
To assess significance, we calculated *p*-values for the following means:

- LNS changes between the two mappings
- Differences between two characteristics
- Differences between LNS in TA and WOT

The level of significance was set at 0.05.
P-values were calculated via the Mann-Whitney U test (for independent samples) and the Wilcoxon test (for related and dependent samples). We used the GraphPad Prism software (GraphPad Prism 6.04, La Jolla, CA, USA) to perform statistical analysis (Ille et al., 2019).

2.6.3.3. FT analysis

After performing nrTMS-based DTI FTs on three occasions (PRE-1, POST-1, and PRE-2), we analyzed fluctuations in the quantity of language conducting fibers on different levels. First, we generated a whole language network tractography by using left-sided LPS gathered in the nrTMS language mapping as ROI seeds. As we used the same ROIs both in the pre- and post-operative DTI FT, we were giving tractography results a function-based starting and end point (Ille et al., 2018). Second, we conducted a subgroup analysis by adding further ROIs to track three specific WMPs: IFOF, FAT, and SLF/AF. Finally, we compared changes in fiber numbers to the individual course of language function.

2.6.4. Visualization

We decided on illustrating the cortical nrTMS data visually to investigate special aspects from a new perspective. For generating images, we chose the Adobe Photoshop software (Adobe Photoshop, 19.1 – 21.2, San José, CA, USA). A template of the CPS by Corina et al. (Corina et al., 2005) served as the background. This background was fused together with the 46 language sites, marked as numbered dots. Special interest was paid to the perisylvian areas, which were outlined in black.
Areas of interest were highlighted in a defined color-coding scheme within additional layers, such as TA, WOT, resected areas, LNS, and LPS to enter individual patient data. In this way, we created one stack of images per hemisphere per mapping and were free to show, hide, or combine different compositions at our discretion to achieve clear visualizations.

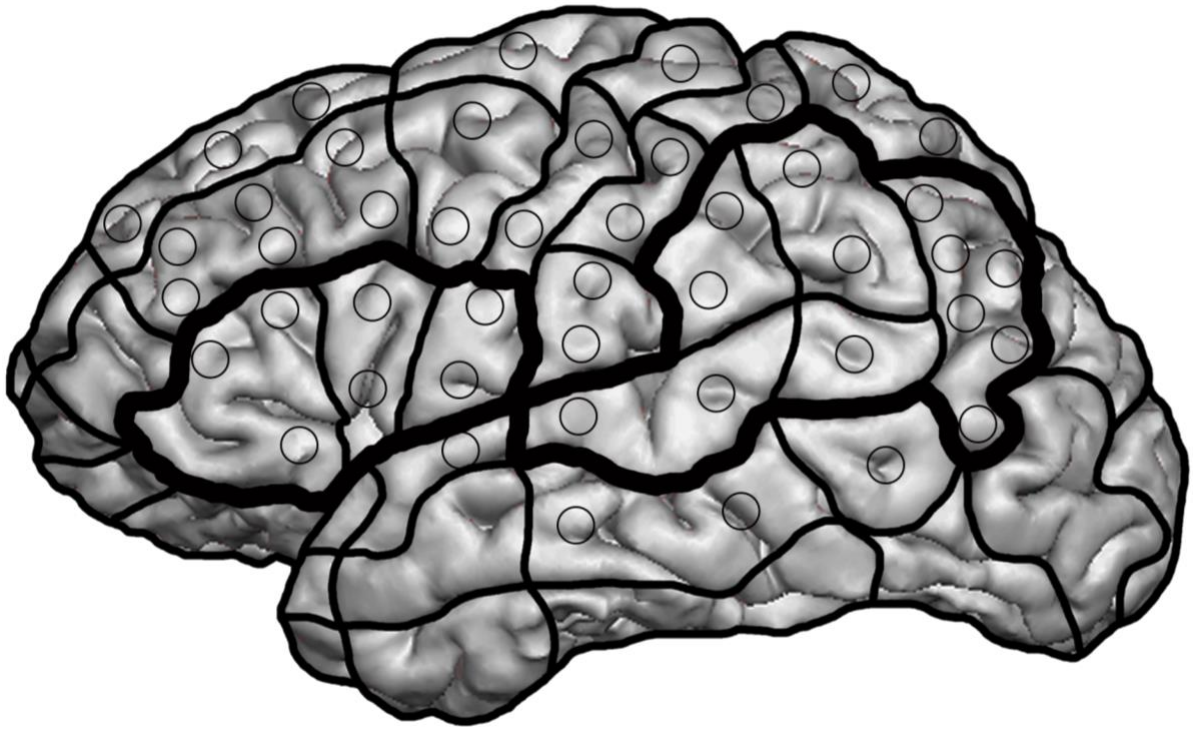

Figure 11 *Universal template*

The universal template before individual color-coding: The cortical parcellation system by Corina et al. (Corina et al., 2005) was combined with the 46 language stimulation sites. Anterior and posterior perisylvian language-related regions are outlined in thick black.

3. RESULTS

3.1. Patient characteristics

We analyzed the medical history of 18 patients with language-affecting gliomas who were treated in the neurosurgical department of the Klinikum rechts der Isar MRI TUM, Munich, Germany. Except for one left-handed and two both-handed patients, the remaining 15 patients were right-handed, as assessed by the EHI. Their ages when diagnosed with glioma ranged from 18 to 74 years of age, with a mean age of 46.2 years.

The observational period ran from January 2013 to September 2017. Each patient received at least two nrTMS language mappings. Second mappings were performed in 15 cases in preparation for another surgery due to tumor recurrence and in three cases as follow-ups (Ille et al., 2019). Every patient underwent awake craniotomy with DES at least one time. We took into account anamnestics on seizures and the intake of anti-epileptic drugs. Language performance was measured on six occasions by using the modified AAT.

ID	Age range	Months between mappings	Seizures before PRE-1/PRE-2	AED	Language performance					
					PRE-1	POD5-1	POM3-1	PRE-2	POD5-2	POM3-2
1	46–50	1	PRE-1	Y	1A	0	–	0	0	0
2	46–50	41	PRE-1	Y	2B	1B	1B	1B	–	–
3	41–45	12	PRE-1 and PRE-2	Y	0	1A	1A	1A	1A	1A
4	18–20	20	N	N	0	0	0	0	2A	0
5	51–55	21	N	N	2B	1B	0	0	0	2A
6	51–55	30	PRE-1	Y	0	0	0	0	–	–
7	51–55	19	PRE-2	N	2A	1A	1A	2A	2A	1A
8	21–25	11	PRE-1	Y	1A	1A	1A	1A	1A	1A
9	31–35	15	PRE-1	Y	1B	1B	0	1A	1A	1A
10	26–30	6	PRE-1	Y	0	0	0	1B	–	–
11	31–35	26	PRE-1	Y	0	1A	0	0	0	0
12	51–55	14	PRE-1 and PRE-2	Y	0	0	0	1B	1B	1B
13	46–50	37	PRE-1	Y	0	1B	0	0	0	0
14	56–60	3	N	N	0	0	0	1A	2A	1A
15	71–75	9	PRE-1	Y	0	0	0	1A	1A	1A
16	36–40	30	PRE-1	Y	0	0	0	0	–	–
17	71–75	13	PRE-1	Y	0	0	0	0	0	0
18	71–75	2	PRE-1	Y	0	2A	0	0	–	–
Mean	46	17								
SD	16	11								

The table shows the characteristics of all included patients (SD, standard deviation; Y, yes, N, no; AED, anti-epileptic drugs; PRE-1, before first surgery, POD5-1, 5 days after first surgery; POM3-1, 3 months after first surgery; PRE-2, before second surgery/evaluation of a second surgery; POD5-2, 5 days after second surgery/evaluation of a second surgery; POM3-2, 3 months after second surgery/evaluation of a second surgery; A, non-fluent aphasia; B, fluent aphasia).

Table 2 Patient characteristics

(Ille et al., 2019)

3.2. Tumor characteristics

During each surgery, tumor samples were taken. A histopathological examination verified that they were all gliomas. Lesions were classified according to the international WHO grading: one oligodendroglioma (OD) and two diffuse astrocytomas (DA). Both entities are subsumed under grade II gliomas. Further, five grade III astrocytomas (AA), nine grade IV glioblastomas (GBM), one primary grade III AA upgraded to a grade IV GBM in the second surgery. Apart from the entity, we gathered information on genetic anomalies of the tumor tissue, such as isocitrate dehydrogenase (IDH) mutation and 1p19q codeletion.

Exactly half of the patients (9) showed lesions that were located in anterior perisylvian areas (A). The other half (9) suffered from lesions affecting posterior areas (P).

Adjuvant treatment after the first surgery was administered in 15 cases by prescribing cytostatic temozolomide. In nine cases, the drug was combined with radiation therapy.

ID	Tumor location	Surgery before PRE1	EOR surgery 1 (%)	EOR surgery 2 (%)	Tumor								
					Surgery 1				Surgery 2				Adjuvant treatment after surgery 1
					Entity	WHO	IDH mutation	1p19q codeletion	Entity	WHO	IDH mutation	1p19q codeletion	
1	P	Y	80	100	GBM	IV	Y	-	GBM	IV	Y	-	N
2	P	N	100	–	AA	III	Y	N	no surgery	–	–	–	TMZ
3	P	N	100	100	GBM	IV	N	–	GBM	IV	N	–	RT/TMZ
4	A	Y	100	70	OD	II	N	–	OD	II	N	N	N
5	P	N	100	100	GBM	IV	–	–	GBM	IV	–	–	RT/TMZ
6	A	N	90	–	AA	III	Y	N	no surgery	–	–	–	TMZ
7	A	N	100	80	GBM	IV	–	–	GBM	IV	–	–	RT/TMZ
8	A	N	100	100	DA	II	Y	N	DA	II	Y	N	N
9	A	Y	100	70	AA	III	Y	N	AA	III	Y	N	TMZ
10	P	N	100	–	GBM	IV	N	–	GBM (Biopsy)	IV	N	–	RT/TMZ
11	A	N	100	100	AA	III	Y	N	AA	III	Y	N	TMZ
12	P	Y	100	100	AA	III	N	N	GBM	IV	N	–	RT/TMZ
13	A	Y	100	100	DA	II	Y	N	DA	II	Y	N	TMZ
14	P	N	100	90	GBM	IV	N	–	GBM	IV	N	–	RT/TMZ
15	P	N	100	100	GBM	IV	N	N	GBM	IV	N	N	RT/TMZ
16	A	Y	100	–	AA	III	Y	N	no surgery	–	–	–	TMZ
17	P	N	100	100	GBM	IV	N	–	GBM	IV	N	–	RT/TMZ
18	A	N	100	80	GBM	IV	N	–	GBM	IV	N	–	RT/TMZ

The table shows tumor characteristics of all included patients (A, anterior; P, posterior; Y, yes; N, no; EOR, extent of resection; GTR, gross total resection; STR, subtotal resection; DA, diffuse astrocytoma; AA, anaplastic astrocytoma; OD, oligodendroglioma; GBM, glioblastoma; RT, radiation therapy; TMZ, temozolomide).

Table 3 *Tumor characteristics*

(Ille et al., 2019)

3.3. Functional reorganization on cortical levels

3.3.1. Language mapping results: ER, HDR, and IHR

A detailed analysis of all nrTMS language mappings with a correlation of ERs, HDRs, and IHRs did not show any trends with statistical significance. However, we noticed a slight increase in IDRs and IHRs after a period of 13 months. These tendencies especially occurred in patients suffering from the slow-growing WHO grade II or III gliomas (Ille et al., 2019).

ID	First mappings								Second mappings								Change of				
	EHI	Error rates		Inter-hemispheric			Intra-hemispheric		EHI	Error rates		Inter-hemispheric			Intra-hemispheric		HDR	aHDR	pHDR	IHR	
		ER-L	ER-R	HDR	aHDR	pHDR	IHR-L	IHR-R		ER-L	ER-R	HDR	aHDR	pHDR	IHR-L	IHR-R				L	R
1	100	0.22	0.15	1.49	1.16	2.86	0.95	2.33	100	0.31	0.18	1.75	1.57	2.92	2.23	4.13	N	N	N	Y	N
2	80	0.10	0.11	0.89	0.55	0.64	1.54	1.80	90	0.23	0.12	1.95	1.88	2.00	1.00	1.07	Y	Y	Y	Y	N
3	100	0.08	0.05	1.67	1.00	0.53	0.43	0.23	100	0.31	0.23	1.34	0.91	0.97	1.01	1.08	N	Y	N	Y	Y
4	60	0.19	0.14	1.42	0.89	3.67	1.81	7.43	60	0.05	0.05	0.93	3.14	2.70	1.74	1.50	Y	N	N	N	N
5	86.7	0.27	0.21	1.27	1.60	1.12	1.66	1.16	86.7	0.10	0.11	0.88	1.02	1.57	1.04	1.59	Y	N	N	N	N
6	100	0.14	0.11	1.26	1.43	2.68	1.26	2.35	100	0.44	0.48	0.91	0.73	0.82	1.29	1.44	Y	Y	Y	N	N
7	100	0.17	0.12	1.42	1.26	1.41	1.52	1.26	100	0.21	0.21	1.04	0.89	1.24	2.17	3.04	N	Y	N	N	N
8	81.1	0.14	0.13	1.04	1.04	0.64	1.45	0.00	81.1	0.19	0.21	0.91	3.91	0.54	1.20	0.16	Y	N	N	N	N
9	30	0.20	n.p.	-	-	-	2.22	-	100	0.10	0.10	1.09	6.56	0.71	2.48	0.27	-	-	-	N	-
10	100	0.16	0.17	0.94	1.02	1.11	1.14	1.23	100	0.18	0.22	0.83	0.14	1.43	0.18	1.90	N	Y	N	Y	N
11	-80	0.15	0.08	1.75	1.76	2.40	1.48	2.02	60	0.02	0.02	1.00	2.86	0.49	5.72	0.98	Y	N	Y	N	Y
12	100	0.11	0.09	1.26	1.67	0.86	1.24	0.64	70	0.10	0.11	0.96	1.38	1.04	1.13	0.84	Y	N	Y	N	N
13	100	0.23	0.17	1.35	1.31	1.82	1.13	1.57	100	0.14	0.12	1.18	3.00	0.77	1.71	0.44	N	N	Y	N	Y
14	56	0.25	0.31	0.79	0.63	0.77	1.06	1.30	56	0.27	0.27	1.00	1.55	0.93	0.89	0.53	Y	Y	N	Y	Y
15	64	0.19	0.13	1.39	1.56	1.10	3.95	2.79	60	0.45	n.p.	-	-	-	1.31	-	-	-	-	N	-
16	20	0.29	0.27	1.06	1.30	1.04	1.90	1.52	40	0.05	0.03	1.81	1.19	1.81	0.78	1.19	N	N	Y	Y	N
17	40	0.05	0.06	0.97	2.28	0.42	2.30	0.42	20	0.17	0.18	0.94	1.64	1.11	2.45	1.67	N	N	N	N	Y
18	90	0.27	0.22	1.18	2.33	0.74	1.59	0.51	90	0.36	0.29	1.22	1.17	0.94	0.99	0.80	N	N	Y	Y	N
Mean	68	0.18	0.15	1.24	1.34	1.40	1.59	1.68	79	0.21	0.17	1.16	1.97	1.29	1.63	1.33					
SD	44	0.07	0.07	0.26	0.48	0.92	0.72	1.63	24	0.13	0.11	0.34	1.50	0.69	1.16	0.97					

Table 4 *Detailed language mapping results*

The table shows detailed language mapping results for every patient, with error rates (ER) for the left (L) and right (R) hemisphere, interhemispheric dominance ratios (HDRs), HDRs for anterior (aHDR) and posterior (pHDR) areas, interhemispheric dominance ratios (IHRs) and changes of these parameters between the first and second mapping (Y = yes; N = no) (Ille et al., 2019).

3.3.2. Language mapping results: LNS

We analyzed the dynamics of LNS over time in relation to the tumor. In cases that had located the most language function near the tumor in the first mapping, an overall increase of LNS in the tumor area during the second mapping was found. This loss of language function within the TA was statistically significant compared to cases without language function near the tumor (p = 0.049) (Ille et al., 2019).

ID	No. of language-negative stimulation sites left hemisphere					
	Tumor area			Area w/o tumor		
	Mapping		More in 2nd mapping	Mapping		More in 2nd mapping
	1	2		1	2	
1	3	6	Y	0	3	Y
2	12	1	N	2	3	Y
3	10	7	N	6	0	N
4	1	1	-	6	10	Y
5	3	7	Y	0	3	Y
6	4	1	N	9	2	N
7	0	1	Y	7	6	N
8	3	2	N	10	7	N
9	0	2	Y	1	8	Y
10	8	4	N	2	5	Y
11	3	2	N	8	13	Y
12	7	4	N	4	4	-
13	0	2	Y	7	10	Y
14	1	1	-	2	1	N
15	8	3	N	1	0	N
16	1	6	Y	5	10	Y
17	10	7	N	7	0	N
18	1	4	Y	6	7	Y

The table shows language-negative stimulation sites within anterior and posterior language-eloquent areas of all patients and mappings (Y, yes; N, no).

Table 5 *Distribution of language-negative stimulation sites on the left hemisphere (Ille et al., 2019)*

Language-negative stimulation sites left hemisphere						
	Tumor area			Area w/o tumor		
Overall	Mapping 1	Mapping 2	Difference	Mapping 1	Mapping 2	Difference
	75	61	-14	83	92	+9
Language near tumor	Mapping 1	Mapping 2	Difference	Mapping 1	Mapping 2	Difference
	26	34	+8	65	76	+11
Language not near tumor	Mapping 1	Mapping 2	Difference	Mapping 1	Mapping 2	Difference
	49	27	-22	18	16	-2
More LNS T area	Mapping 1	Mapping 2	Difference	Mapping 1	Mapping 2	Difference
	8	28	+20	26	47	+21
Less LNS T area	Mapping 1	Mapping 2	Difference	Mapping 1	Mapping 2	Difference
	65	31	-34	49	34	-15
Aphasia POD5-1	Mapping 1	Mapping 2	Difference	Mapping 1	Mapping 2	Difference
	32	28	-4	47	57	+10
No aphasia POD5-1	Mapping 1	Mapping 2	Difference	Mapping 1	Mapping 2	Difference
	43	33	-10	36	35	-1
Surgery-related deficit	Mapping 1	Mapping 2	Difference	Mapping 1	Mapping 2	Difference
	14	15	1	27	30	3
Tumor-related deficit	Mapping 1	Mapping 2	Difference	Mapping 1	Mapping 2	Difference
	45	33	-12	35	31	-4
Seizures	Mapping 1	Mapping 2	Difference	Mapping 1	Mapping 2	Difference
	70	52	-18	75	78	3
No seizures	Mapping 1	Mapping 2	Difference	Mapping 1	Mapping 2	Difference
	5	9	4	8	14	6

Table 6 *Language-negative stimulation sites depending on different characteristics (Ille et al., 2019)*

		Tumor area					Area w/o tumor					Tumor area vs. area w/o tumor
		Mapping 1	Mapping 2		Difference		Mapping 1	Mapping 2		Difference		
Language near tumor	Total	26	34	$p = 0.41$	+8	$p = 0.049$	65	76	$p = 0.50$	+11	$p = 0.36$	$p = 0.86$
	Mean	2.4	3.1		0.7		5.9	6.9		1		
Language not near tumor	Total	49	27	$p = 0.17$	−22		18	16	$p > 0.99$	−2		$p = 0.31$
	Mean	7	3.9		−3.1		2.6	3.3		−0.3		
Aphasia POD5-1	Total	32	28	$p = 0.77$	−4	$p = 0.42$	47	57	$p = 0.40$	+10	$p = 0.62$	$p = 0.77$
	Mean	3.6	3.1		−0.4		5.3	6.2		1.1		
No aphasia POD5-1	Total	43	33	$p = 0.44$	−10		36	35	$p > 0.99$	−1		$p = 0.55$
	Mean	4.8	3.7		−1.1		4	3.9		−0.1		
Surgery-related deficit	Total	14	15	$p = 0.14$	1	$p = 0.25$	27	30	$p > 0.99$	3	$p = 0.63$	$p = 0.24$
	Mean	4.9	3.1		−1.7		3.3	3.4		1.4		
Tumor-related deficit	Total	45	33	$p > 0.99$	−12		35	31	$p = 0.88$	−4		$p > 0.99$
	Mean	3.5	3.8		0.3		6.8	7.5		0.8		
Seizures	Total	70	52	$p = 0.30$	−18	$p = 0.28$	75	78	$p = 0.82$	3	$p = 0.59$	$p = 0.31$
	Mean	4.7	3.5		−1.2		5	5.2		0.2		
No seizures	Total	5	9	$p > 0.99$	4		8	14	$p = 0.50$	6		$p > 0.99$
	Mean	1.7	3		1.3		2.7	4.7		2		

The table shows overall language-negative stimulation sites (LNS) of the left hemisphere in dependence on different characteristics (POD5-1 = 5 days after first surgery).

Table 7 *P-values of language-negative stimulation sites and different characteristics (Ille et al., 2019)*

3.3.3. Illustrative case: Patient 13

This male patient was diagnosed at the age of 43 years in 2007 with a left-sided hisotpathologically confirmed DA (WHO grade II) with IDH mutation. Having an EHI of 100%, he was classified as a strong right-hander.

At first, remission was obtained by surgical and conservative treatment, including chemotherapy and radiotherapy. Due to a history of seizures, the patient was receiving AEDs. Unfortunately, a follow-up MRI scan at the beginning of 2013 showed a tumor recurrence in the left temporal lobe and the insula. This tumor was spreading periventricularly. The CPS regions that were mainly affected were the aSTG, mSTG, and opIFG, with partial infiltration of the aMTG and mMTG. Thus, we classified the lesion as both A and P. So far, the patient has not presented with any language impairment. He reached a value of 0 on the AAT. He also was not suffering from any motor deficit or impairment of further cognitive function.

Surgical removal of the tumor was planned. Therefore, we performed a preparatory nrTMS language mapping.

As the location of the lesion bore a high risk of injuring the language network during resection, a partially awake surgical approach with DCS was chosen. Intraoperatively, the vPrG was detected as language-positive, which confirmed the nrTMS mapping result. An EOR of 100% was achieved.

In the POD5-1 examination, a transient fluent aphasia, grade 1B according to the AAT, was observed. The impairment did improve quickly, as the patient again presented with no residual aphasia in the POM3-1 follow-up. After surgery, he received temozomide as adjuvant treatment.

The remission lasted nearly three years, at which time the patient was again admitted to our department due to tumor recurrence in the frontal lobe. This time, mainly the trIFG and opIFG were affected along with partial infiltration of the vPrG, pMFG, and mMFG. The tumor mass did relate to the former resection cavity. Once more, a preoperative nrTMS language mapping (37 months after the first one) and consecutive DCS during awake craniotomy were performed. An EOR of 100% was achieved. Intraoperatively, the vPrG was again confirmed as language positive, which again matched the nrTMS mapping results. Neither at PRE-2 nor POD5-2 language impairment was described.

A comparison of the results of both nrTMS language mappings revealed an increase of LNS within anterior and posterior language-eloquent areas of the left hemisphere. This trend happened in the TA (from 0 to 2 LNS) and the WOT (from 7 to 10 LNS). Simultaneously, LNS in the right hemisphere decreased over time (from 18 to 12 LNS).

In the first mapping, a left-hemispheric and anteriorly located language dominance was detected with an HDR of 1.35 and a left-sided IHR of 1.13. There was no new trend concerning

these ratios in the second mapping due to especially high ERs at single stimulation sites (HDR 1.18; IHR 1.71). (Ille et al., 2019)

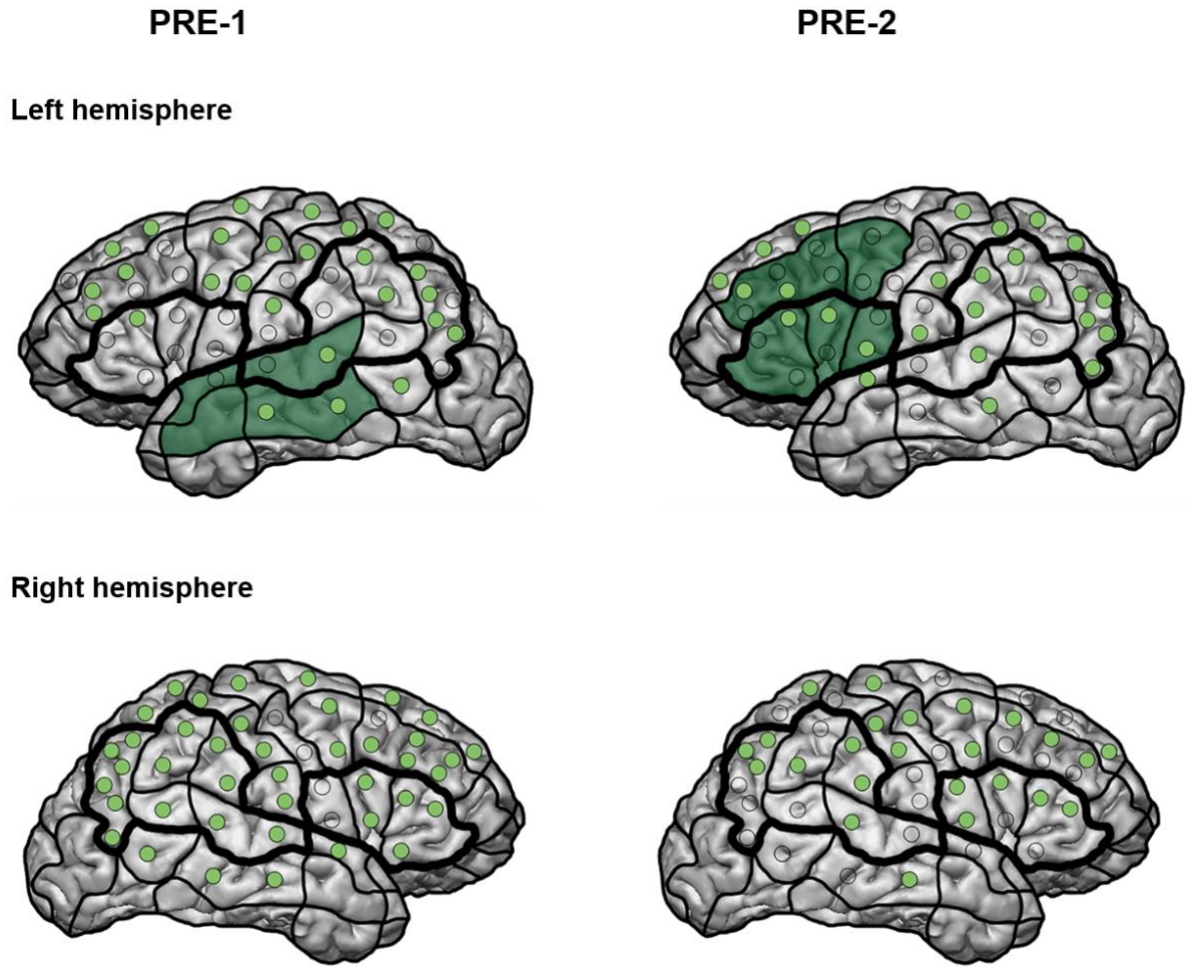

Figure 12 *Visualization of language negative sites and the tumor area in patient 13*

Language-negative sites (LNS) as measured by navigated repetitive transcranial magnetic stimulation language mapping in patient 13 prior to the 1st and 2nd surgery (PRE-1 and PRE-2). Anterior and posterior language-related regions are outlined in black. LNS are highlighted in light green, whereas the tumor area on the left hemisphere is shaded in dark green. Overall, LNS increased over time in perisylvian areas on the left hemisphere while decreasing on the right hemisphere.

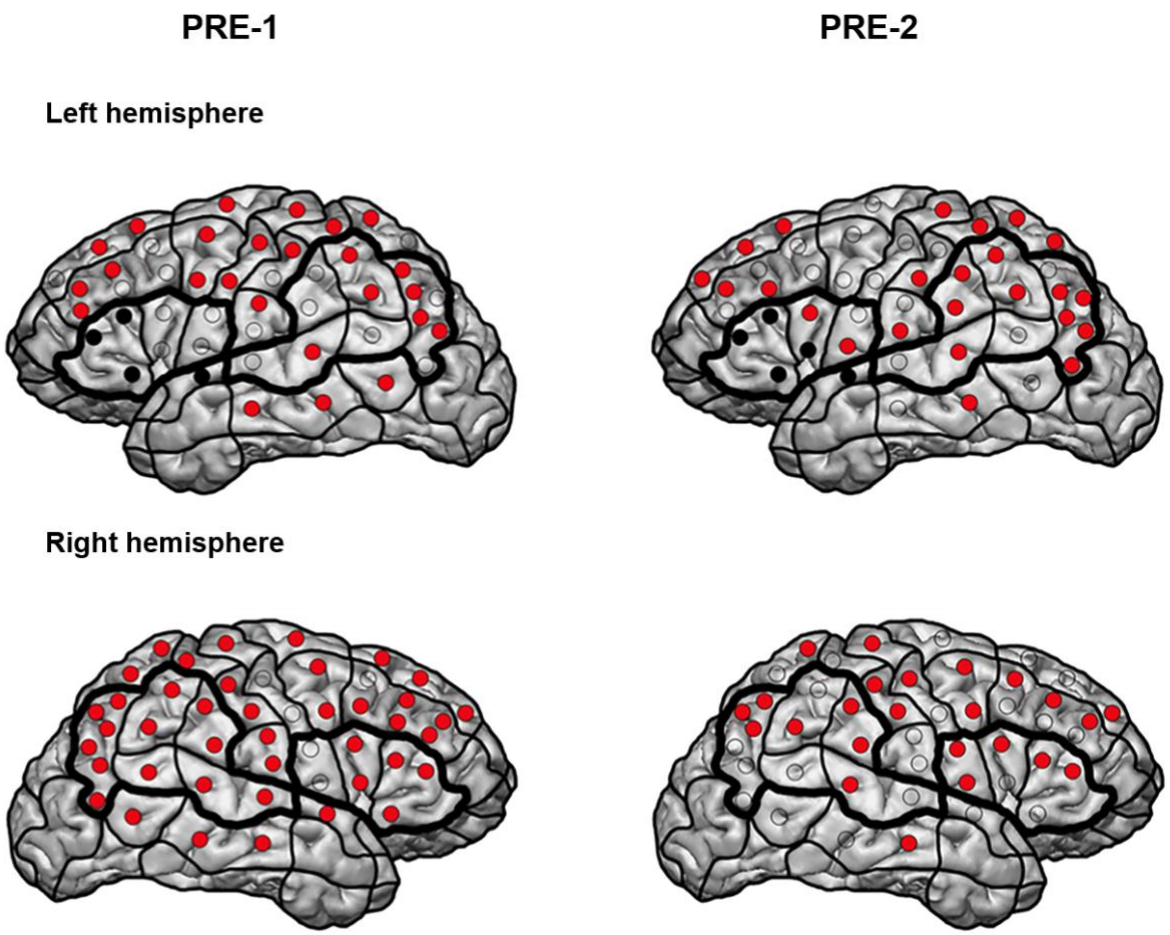

Figure 13 *Visualization of language negative sites and resected areas in patient 13 Language-negative sites (LNS) as measured by nrTMS language mapping in patient 13 prior to the 1st and 2nd surgery (PRE-1 and PRE-2). Anterior and posterior language-related regions are outlined in black. LNS are highlighted in red, whereas resected areas are colored black (Ille et al., 2019).*

3.4. Functional reorganization on subcortical levels

3.4.1. FT patient characteristics

A sufficient comparison of fibers was possible in ten patients (patient IDs: 3, 5, 9, 11, 12, 13, 14, 16, 17, and 18).

Clearly, the smaller cohort changed the characteristics of this patient sample.

The mean age was four years older than in the primary sample. Out of the ten included patients, three were female and seven were male (Ille et al., 2018).

Patient	Age	PRE-1 to PRE-2 (months)	PRE-1 to 2nd DTI (days)	PRE-1 to 3rd DTI (months)	Subcortical ischemia after surgery 1	EOR	Aphasia grading						Course of language function
							PRE-1	POD5-1	POM3-1	PRE-2	POD5-2	POM3-2	
3	45	12	15	6	N	GTR	0	1A	1A	1A	–	–	Permanent surgery-related deficit
11	34	26	7	26	Y	GTR	0	1A	0	0	0	0	Transient surgery-related deficit
13	49	37	189	25	Y	GTR	0	1B	0	0	–	–	Transient surgery-related deficit
18	74	2	57	2	N	GTR	0	2A	0	0	–	–	Transient surgery-related deficit
9	31	15	1	14	N	GTR	1B	1B	0	1A	1A	1A	New tumor-related deficit
12	51	14	3	14	N	GTR	0	0	0	1B	1B	1B	New tumor-related deficit
14	56	3	5	3	N	GTR	0	0	0	1A	2A	1A	New tumor-related deficit
5	52	21	120	22	N	GTR	2B	1B	0	0	0	2A	Without new deficit
16	36	30	13	28	N	GTR	0	0	0	0	–	–	Without new deficit
17	72	13	7	13	N	GTR	0	0	0	0	0	0	Without new deficit

The table shows detailed patient characteristics of all included patients including the intervals between the different MR images, the status of language function at each examination, and the assignment of patients to different subgroups (Y, yes, N, no; EOR, extend of resection, GTR, gross total resection).

Table 8 *Patient characteristics and aphasia grading in the fiber-tracking cohort (Ille et al., 2018)*

3.4.2. FT tumor characteristics

Due to the smaller sample, the composition of tumor characteristics was different. Still, the ratio between anterior (A = 50%) and posterior tumors (P = 50%) remained consistent, with five patients each. As this analysis aimed to take a closer look at WMPs, we calculated the ratio of tumor volume between subcortical and cortical levels. In seven out of ten patients, more than 50% of the tumor mass was located in subcortical areas (Ille et al., 2018).

Patient	Surgery before PRE-1	Tumor						Recurrence at PRE-2
		Entity	WHO grade	IDH mutation	1p19q codeletion	Location	Subcortical	
3	N	GBM	IV	N	–	aSMG	N	N
11	N	AA	III	Y	N	insular	Y	Y
13	Y	DA	II	Y	N	insular	Y	N
18	N	GBM	IV	N	-	mMFG/pMFG	Y	Y
9	Y	AA	III	Y	N	pMFG/opIFG	Y	Y
12	Y	AA	III	N	N	pMTG	N	Y
14	N	GBM	IV	N	–	aSMG	N	Y
5	N	GBM	IV	–	–	STG	Y	Y
16	Y	AA	III	Y	N	pMFG/opIFG	Y	N
17	N	GBM	IV	N	–	STG	Y	Y

The table shows the tumor characteristics of all included patients and the detailed location of each tumor (Y, yes, N, no; DA, diffuse astrocytoma, AA, anaplastic astrocytoma, GBM, glioblastoma; aSMG, anterior supramarginal gyrus, mMFG, middle middle frontal gyrus; pMFG, posterior middle frontal gyrus; opIFG, opercular inferior frontal gyrus; pMTG, posterior middle temporal gyrus; STG, superior temporal gyrus).

Table 9 *Tumor characteristics in the fiber-tracking cohort (Ille et al., 2018)*

3.4.3. Fiber tracking analysis

3.4.3.1. Single white-matter-pathway analysis

Overall, changes in fiber quantity showed a strong positive correlation with the progression of aphasia. This applied to subgroups of fibers and the total number of fibers.
(Ille et al., 2018)

Patient	Number of fibers at PRE-1				AG	% Difference between PRE-1 and POST-1				LF	% Difference between POST-1 and PRE-2				LF	% Difference between PRE-1 and PRE-2				LF
	IFOF	FAT	SLF/AF	Total		IFOF	FAT	SLF/AF	Total		IFOF	FAT	SLF/AF	Total		IFOF	FAT	SLF/AF	Total	
1	567	2890	3934	7391	0	−85.9	−83.1	−67.5	−75.0	W	1866.3	−22.9	−36.7	49.4	U	177.4	−87.0	−79.4	−62.7	W
2	833	483	2982	4298	0	−37.2	−93.2	−78.8	−72.4	W	−99.0	648.5	29.4	−9.9	I	−99.4	−48.9	−72.6	−75.1	U
3	392	86	274	752	0	−66.8	−100	−26.6	−56.0	W	0.8	–	102.5	76.1	I	−66.6	−47.7	48.5	−22.5	U
4	124	3	4223	4350	0	−98.4	−100	−99.4	−99.4	W	1700.0	–	2215.4	2192.9	I	−71.0	33.3	−85.7	−85.2	U
5	51	0	38	89	1B	−23.5	–	189.5	82.0	U	1564.1	−69.2	−100	303.1	W	1172.5	–	−100	633.7	W
6	2150	6	8499	10655	0	−78.9	−100	−95.9	−92.4	U	−96.3	–	−98.3	−97.1	W	−99.2	−100	−99.9	−99.8	W
7	8747	1522	6588	16857	0	−86.7	−61.8	−97.3	−88.6	U	−99.5	−100	−84.8	−98.3	W	−99.9	−100	−99.6	−99.8	W
8	416	0	2231	2647	2B	−98.3	–	−17.3	−23.6	U	14471.4	−43.9	49.8	91.8	U	145.2	–	23.8	46.5	U
9	109	110	682	901	0	138.5	−100	−76.7	−53.5	U	573.1	–	1059.7	758.0	U	1505.5	−99.1	170.4	299.0	U
10	201	0	62	263	0	613.4	–	7466.1	2228.9	U	−85.5	–	−41.0	−43.3	U	3.5	–	4366.1	1220.5	U

The table shows the absolute number of fibers for each of the separately tracked subcortical pathways at PRE-1, the initial aphasia grading at PRE-1, and the percentage changes of nrTMS-based DTI FTs between PRE-1 and POST-1, POST-1, and PRE-2, and PRE-1, and PRE-2 as well as the changes of language function in all patients. The table also shows the correlation of the course of language function in each patient and the according difference of fibers of each single white matter pathway. Percentages highlighted in green indicate a correlation of the percentage changes of single white matter pathways and the according course of language function. Percentages highlighted in red indicate a lack correlation of the percentage changes of single white matter pathways and the according course of language function (AF, aphasia grading at PRE-1, LF, language function; W, worsened; U, unchanged; I, improved).

Table 10 *Course of absolute and relative fiber numbers in total and for single pathways (Ille et al., 2018)*

3.4.3.2. Subgroup Analysis

Once we had assorted the patients into different subgroups of language impairment, we counted the overall change of fibers in absolute numbers and percentage-wise for every group. We noticed the following:

1. In the four patients with a new surgery-related language deficit at POST-1 (irrelevant, permanent, or transient), a total loss in overall fibers of −79.8% in all pathways (IFOF, FAT, and SLF/AF) occurred.
2. The one patient with a permanent surgery-related language deficit showed a gain in overall fibers of +49.4% between POST-1 and PRE-2. While the IFOF gained a remarkable amount of fibers, +1,866.3%, FAT and SLF/AF showed losses of −22.9% and −36.7%, respectively.

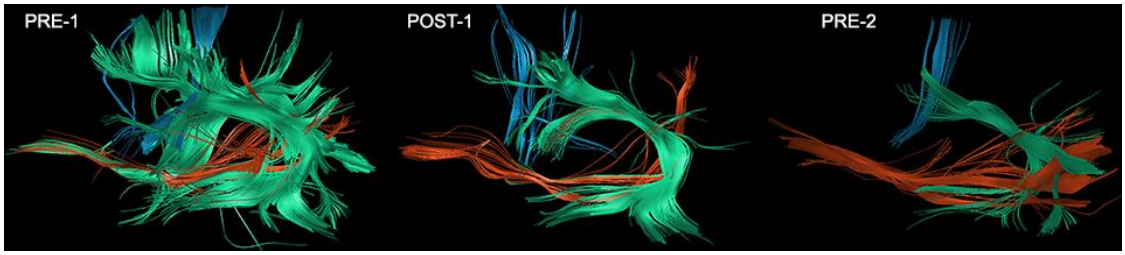

Figure 14 *White matter pathway changes after a permanent surgery-related deficit*
This figure shows the changes in the inferior fronto-occipital fascicle (IFOF, shown in red), the superior longitudinal fascicle and arcuate fascicle (SLF/AF, shown in green),

and the frontal aslant tract (FAT, shown in blue) in patient 3, who suffered from a permanent surgery-related language deficit grade 1A according to the Aachener Aphasia Test (AAT) (Ille et al., 2018).

3. The three patients with a transient surgery-related language deficit gained a similar amount of fibers, with +48.4% more fibers in PRE-2 than in POST-1. Especially, the FAT showed a big increase of +797.0% more fibers, while the IFOF decreased by −73.7%. The SLF/AF increased slightly by +112.7%.
4. In the three patients who suffered from a new tumor-related language deficit in PRE-2, an overall loss of fibers occurred, not only between POST-1 and PRE-2 (−89.5%) but also between PRE-1 and POST-1 (−75.5%).

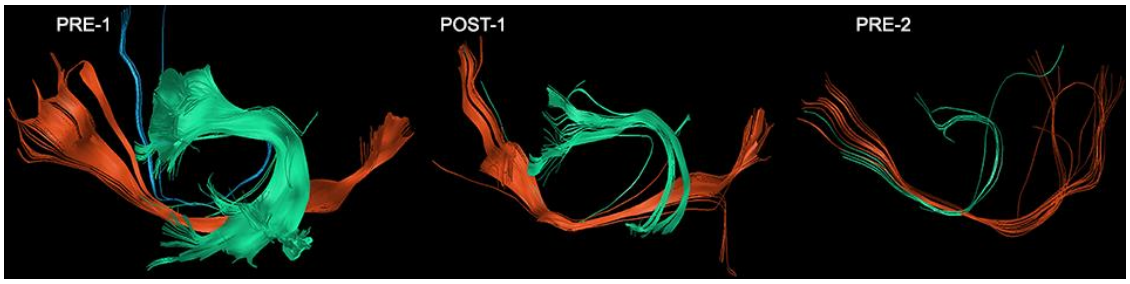

Figure 15 *White matter pathway changes after a tumor-related language deficit*
This figure shows the changes in the inferior fronto-occipital fascicle (IFOF, shown in red), the superior longitudinal fascicle and arcuate fascicle (SLF/AF, shown in green), and the frontal aslant tract (FAT, shown in blue) in patient 12, who suffered from a new tumor-related language deficit grade 1B, according to the Aachener Aphasia Test (AAT).

5. The remaining three patients **without new language deficits** showed a constant increase of fibers, with +124.8% between PRE-1 and POST-1 and +27.8% between POST-1 and PRE-2

(Ille et al., 2018).

	IFOF	FAT	SLF/AF	Total
DIFFERENCE BETWEEN PRE-1 AND POST-1 IN NEW SURGERY-RELATED LANGUAGE DEFICITS				
Relative	−61.6%	−84.9%	−81.3%	−79.8%
Absolute	−1181	−2940	−9275	−13,396
Mean	−295.3	−735.0	−2,318.8	−3,349.0
SD	130.5	976.4	1,473.5	1,896.8
DIFFERENCE BETWEEN POST-1 AND PRE-2 IN PERMANENT SURGERY-RELATED LANGUAGE DEFICIT				
Relative	1,866.3%	−22.9%	−36.7%	49.4%
Absolute	1493	−112	−469	912
DIFFERENCE BETWEEN POST-1 AND PRE-2 IN TRANSIENT SURGERY-RELATED LANGUAGE DEFICITS				
Relative	−73.7%	797.0%	112.7%	48.4%
Absolute	−483	263	968	748
Mean	−161.0	87.7	322.7	249.3
SD	252.8	90.9	179.3	298.8
DIFFERENCE BETWEEN PRE-1 AND POST-1 IN NEW TUMOR-RELATED LANGUAGE DEFICITS				
Relative	−84.9%	−61.1%	−95.8%	−89.5%
Absolute	−9,290	−933	−14,486	−24,709
Mean	−3,096.7	−311.0	−4,828.7	−8,236.3
SD	3,245.3	444.8	4,332.2	6,231.1
DIFFERENCE BETWEEN POST-1 AND PRE-2 IN NEW TUMOR-RELATED LANGUAGE DEFICITS				
Relative	−59.5%	−99.3%	−94.8%	−75.5%
Absolute	−986	−591	−606	−2,183
Mean	−328.7	−197.0	−202.0	−727.7
SD	726.2	272.3	102.5	973.6
DIFFERENCE BETWEEN PRE-1 AND POST-1 IN PATIENTS WITHOUT NEW LANGUAGE DEFICIT				
Relative	134.3%	55.5%	125.0%	124.8%
Absolute	975	61	3,719	4,755
Mean	325.0	20.3	1239.7	1,585.0
SD	681.5	115.6	2,397.3	3,024.9
DIFFERENCE BETWEEN POST-1 AND PRE-2 IN PATIENTS WITHOUT NEW LANGUAGE DEFICIT				
Relative	75.1%	246.8%	10.2%	27.8%
Absolute	1,277	422	682	2,381
Mean	425.7	140.7	227.3	793.7
SD	1,184.0	253.2	1,551.6	2,495.2

The table shows the summarized changes of single white matter pathway fibers for the different subgroups of patients.

Table 11 *Fiber number changes of single white matter pathways for different subgroups (Ille et al., 2018)*

4. DISCUSSION

4.1. Overview and objectives

Overall, our results confirm that FR of LNS in patients suffering from eloquent gliomas can be detected by nrTMS language mapping (Ille et al., 2019). This study is an expansion of previous research since it has already been confirmed that nTMS can observe cortical FR of motor eloquent areas in glioma patients (Conway et al., 2017).

Moreover, we verified that the number of fibers in the IFOF, FAT, and SLF/AF, as determined by an nrTMS-based DTI FT, correlates positively with the individual course of language function. This phenomenon was observed consistently at PRE-1/2, POD5-1/2, and POM3-1/2 (Ille et al., 2018).

4.2. Measuring functional reorganization on cortical levels via nrTMS

4.2.1. Significance of language-negative sites

Previous research on nrTMS language mappings has repeatedly established the significance of analyzing LNS. Compared to the gold-standard technique of DES, nrTMS is sensible but unspecific in detecting LPS. A study that compared the effectiveness of preoperative language mapping to DES during the subsequent awake craniotomy found a sensitivity of 90.2%, specificity of 23.8%, positive predictive value of 35.6%, and negative predictive value of 83.9% (Picht et al., 2013). Afterward, similar numbers were described in several publications (Ille et al., 2015a; Krieg et al., 2014b; Tarapore et al., 2013). Consequently, we also decided to focus on LNS rather than LPS. This was sensible since this approach would facilitate the comparability of our study to previous research.

4.2.2. Interpretation of results

Overall, our results support findings from previous publications, as we found nrTMS can indeed measure functional reorganization in glioma patients (Conway et al., 2017; Krieg et al., 2013; Rosler et al., 2014).

Concerning our more detailed analysis regarding different characteristics, one connection, in particular, stood out. In patients who had shown a close proximity between language eloquent areas and the tumor area in the first mapping, the number of LNS near the tumor area had increased by the second mapping. This finding suggests that function had moved away from the lesion. This trend of FR showed statistical significance (p = 0.049) compared to patients whose function had not been located near the tumor initially.

If language function was moving away from the lesion, we wondered where it settled. One plausible possibility is that it migrated to the contralateral hemisphere. However, in comparing hemispheric dominance ratios, we could debunk this hypothesis. Surprisingly, the opposite had happened. In only 29% of patients with more LNS near the tumor area in the second mapping, a swap of hemispheric dominance ratios had occurred, whereas something different happened in patients with a decrease of LNS near the tumor. In these cases, we found a change of hemispheric dominance in 56% of patients. We postulated the following theory to describe this observation: If a language eloquent area was directly affected by either the infiltrating glioma itself or its surgical resection, the function would pool in fewer eloquent sites. But, if the language network was untouched, its configuration would remain widespread.

We could support this theory with another observation. Five of our patients were presenting with a new surgery-related language deficit in POD-1 (one permanent and four transient). These patients showed an overall increase of LNS, both in the tumor area and the WOT, along with consistent HDRs in four out of five cases. All of these patients received a subsequent treatment in a rehabilitation clinic between POD-1 and PRE-2 to intensively treat this new deficit. It is likely that the extra support these patients received affected FR differently than other patients.

In patients with a new tumor-related language deficit in PRE-2, we observed a different trend. These patients showed overall less LNS in the second mapping. We hypothesized that FR was triggered by the growing lesion; thus, function spread widely to avert an imminent loss.

Indeed, time seems to play a significant role in FR processes. This assumption was born from a couple of observations. First, five out of the six patients with a tumor-related language deficit suffered from rapidly growing recurrent WHO grade IV glioblastomas. Similar to a sudden surgical trauma, time seemed to be lacking to compensate for the loss by reorganization, leading to aphasic symptoms. Alternatively, we found an increase of FR in low-grade glioma patients and in patients with a long tumor-free survival (cut-off at 13 months). Second, as IHRs and HDRs increased, more time elapsed between mappings. This phenomenon also suggests that time is of the essence in regard to functional reorganization.

(Ille et al., 2019)

4.2.3. Integration into current knowledge on cortical plasticity

As previously mentioned, the gold-standard technique for locating language-positive areas is DES. Thus, the reliability of other non-invasive mapping techniques is always rated in relation to DES. We were pleased that our significant key result—language eloquent areas decreasing around the tumor area—was confirmed by a large-scale DES study. The neurosurgical department at the University of California published a paper in 2016 in which they compared over 500 patients with eloquent gliomas who had undergone iterative awake craniotomy. They

found that cortical areas adjacent to the tumor lost functionality, decreasing from 18.8% LPS at the time of the first surgery to 12.0% during the second surgery. These changes occurred without any new neurological impairment, suggesting preservation of function by FR (Southwell et al., 2016). While the study of Southwell et al. faced the bias of spatial limitation, as an ideal craniotomy is sized as small as possible, we had the advantage of observing the whole cortex using nrTMS as a noninvasive mapping technique.

Furthermore, a number of studies have reported similar trends. These studies, which have had fewer patients, compared DES, fMRI, and nTMS in varying constellations (Duffau et al., 2002; Hayashi et al., 2014; Krieg et al., 2014a; Robles et al., 2008).

Our observation of a higher incidence of severe aphasia in patients with high-grade gliomas is supported by various publications. The 2010 paper of Keidel et al. compared patients with large low-grade gliomas showing no impairment to patients suffering from small high-grade gliomas presenting with severe loss of function. Plastic processes seem to have no chance of overcoming the damages caused by rapidly growing gliomas. It is suggested that the nature of FR depends on three different principles: patterns of connectivity; experience-dependent plasticity; and the time course of damage (Keidel et al., 2010). Other publications addressing this issue emphasize that patients with slow-growing lesions recover faster, have a higher EOR and a better ipsilateral and contralateral recruitment of formerly noninvolved brain areas (Desmurget et al., 2007; Szalisznyo et al., 2013). Especially, this migration of function toward the non-dominant hemisphere has been repeatedly reported in glioma patients (Krieg et al., 2013; Rosler et al., 2014). Again, all these studies support our result, indicating that an increasing amount of language function shifts to the right hemisphere as the observational period increases.

4.3. The number of language eloquent fibers reflects the course of language function

4.3.1. Results

In general, our results show a strong correlation between the overall number of fibers and the course of language function. In cases of newly occurring language deficits, results were especially reliable.

This trend remained consistent in our subgroup analysis regarding the IFOF, FAT, and SLF/AF. Different forms of aphasia correlated with a relatively isolated loss of fibers in their corresponding WMPs. Similar results had already been published in previous studies, as compiled in the 2015 review by Chang et al. (Chang et al., 2015). Patients suffering from non-fluent aphasia presented with a decrease of fibers in the SLF/AF and FAT. These pathways account for the major part of the dorsal stream in the dual stream model and are known to be

crucial in maintaining and acquiring language skills. The occurrence of fluent aphasia accompanied a decrease of fibers in the IFOF, the main pathway of the ventral semantic stream.

We found an average fiber loss of −79.8% in the event of new surgery-related deficits between PRE-1 and POST-1. If the deficit was transient, patients showed a subsequent gain in fiber quantity by PRE-2. Even the patient with a permanent deficit showed a gain in fibers, although he did not completely regain his previous numbers from PRE-1. Interestingly, he gained IFOF fibers exclusively, while he continued to lose fibers in the SLF/AF and FAT. His clinical findings matched these changes, as he suffered from non-fluent aphasia, which is typical for impairments of these pathways.

In the three cases of new tumor-related deficits, we found a fiber deficit of −75.5% from POST-1 to PRE-2. However, two of these patients had already lost fibers between PRE-1 and POST-1 without presenting any surgery-related aphasic symptoms.

By contrast, patients that did not suffer from language deficits during the observational period lost fibers during surgery and regained them by the PRE-2 follow-up (Ille et al., 2018).

4.3.2. The role of white matter pathways in neuroplasticity

Recently, an increasing number of researchers have agreed that WMPs are the main limitation of functional reorganization. Even though minute damage to WMPs can cause major functional impairments, large-scale cortical resections are possible without any loss of function (Duffau, 2014; Ius et al., 2011; Picart et al., 2019).

Our results confirm this previous research, as we have found a high correlation between changes in the numbers of fibers of single WMPs and the individual course of language function. Since we used the same ROIs in the PRE-1 and POST-1 DTI FTs, we were able to exclude cortical changes as the cause of fiber development between PRE-1 and POST-1.

However, the behavior of intact WMPs remains poorly understood.

By the use of non-invasive examinational techniques, such as fMRI and DTI FT, changes on a subcortical level following a lesion have already been observed. The resulting data, including the present study, certainly prove that the language network, as a whole, is able to compensate for damage to white matter. Several supportive mechanisms have been proposed: unmasking of perilesional latent networks, recruitment of accessory pathways, the introduction of additional relays within the circuit, and involvement of parallel, long-distance association pathways (Duffau, 2006, 2009; Fischer et al., 1997; Kong et al., 2016). The existence of these mechanisms could explain our observation of the fiber increase between POST-1 and PRE-2 in our patients with transient surgery-related deficits (Ille et al., 2018).

Moreover, our results indicate that damage on a subcortical level is not necessary for the induction of white-matter plasticity. Four of our patients suffered from a new surgery-related

deficit in POST-1. In each case, the deficit was reflected by a loss of fibers in every tracked pathway. Only two patients presented with subcortical ischemia in the postoperative MRI. This led us to conclude that subcortical reorganization might also occur as a reaction to cortical changes. One reason for the loss of fibers in the two patients without any subcortical damage might be the loss of connectivity to damaged cortical areas. Another indicator that this is the case is the fact that we used the same LPS as ROIs in the fiber trackings at PRE-1 and POST-1. Later, in POM3-1, both patients had completely recovered from their impairment, perhaps because of efficient subcortical reorganization.

In cases of a tumor recurrence, patients presented differently: While three patients suffered from a new language impairment and had fiber loss, we did not record any changes in the other four patients. Apparently, a degree of impairment exists, at which the language network as a whole is no longer able to compensate for damage and preserve function (Ille et al., 2018).

4.3.3. Error sources of DTI FT

At several points in time, we noticed sudden mismatches between fiber numbers and the course of language function when compared to our overall results. These mismatches peaked at different times, depending on which DTI FT approach we used.

Concerning nrTMS-based DTI FT, the mismatch occurred right after surgery. The three concerned patients (9, 12, and 14) did not suffer from a new surgery-related language impairment but seemed to have a substantial loss in fibers. The one aspect these patients had in common was a rather short interval between PRE-1 and the DTI imaging at POST-1. We concluded that postoperative edema might impair DTI imaging. This theory was supported by four patients (3, 11, 13, 18) who suffered from a new surgery-related language deficit in POST-1. These patients had longer intervals between PRE-1 and POST-1, and their change in fiber numbers correlated well with the course of language function, both overall and for each WMP. Regarding the specific analysis of single WMPs, fiber numbers and language function correlated in 63% of cases in POST-1 and 80% of cases at PRE-2. Again, the overall mismatch at POST-1 likely occurred because of postoperative edema, which affected the DTI imaging. Upon closer examination of the mismatch at PRE-2, we noticed the following: In three patients (3, 9, and 11) who suffered from non-fluent aphasia, the mismatch occurred mainly due to fiber changes in the IFOF. However, the IFOF, as part of the ventral stream, conducts mainly semantic information. Impairments in this stream are known to result in fluent aphasia. Once we disregarded the IFOF numbers in our calculations for these three patients, the mismatch in PRE-2 shrunk from 20% to 10%

(Ille et al., 2018).

4.4. Future perspectives: utilization of functional reorganization for the treatment of eloquent gliomas

The main aim in treating eloquent gliomas is the preservation of function. In contrast, a glioma resection strives to be as extensively as possible, to achieve a good clinical outcome. Recently, it has been repeatedly emphasized that a vast EOR is crucial for minimizing recurrence and prolonging survival (Duffau, 2013; Hervey-Jumper and Berger, 2016). Balancing these two competing goals is done through a close examination of the patient's individual characteristics (Duffau and Mandonnet, 2013; Mandonnet and Duffau, 2018).

Recently, nTMS-based DTI FT turned out to be a promising tool to assess individual risk for motor dysfunction in glioma patients (Sollmann et al., 2018).

Our present study has proven once again that reorganization of language eloquent areas is indeed happening in glioma patients. If FR could be actively induced preoperatively and functional areas guided away from the tumor, the resection of a larger region could safely be conducted without jeopardizing eloquent areas. This approach could lead to a better functional outcome and a lower recurrence rate. Currently, such a directed utilization of FR is still open for debate.

Nonetheless, initial steps in this direction have already been taken. In patients for who the maximum EOR is not possible, a multistage surgical approach is suggested. In gradually extending resection toward functional areas by conducting several surgeries, plasticity is induced, and function is relocated. Thus, larger resections are possible without any impairment in abilities (Duffau, 2014; Martino et al., 2009; Robles et al., 2008). A large-scale study has demonstrated that "more efficient plasticity mechanisms are facilitated by cortical tumors with sharp borders" since EORs could be increased at reoperation, and earlier recovery of function was possible (Picart et al., 2019).

Rather than waiting for an internal stimulus to initiate FR (e.g., glioma or surgery), perhaps TMS could be used as a pre-rehabilitation technique to induce plasticity in advance by repetitively placing virtual lesions near at-risk eloquent areas (Pascual-Leone et al., 2000).

4.5. Limitations

4.5.1. Overall limitations

Clearly, our relatively small cohort of 18 patients in the cortical nrTMS study and only ten patients in the FT analysis might constitute a limitation. Accordingly, subgroup numbers were even smaller. However, our small-sized cohort makes our significant key result of language function, leaving the tumor area even more outstanding. However, it would be reasonable to confirm our results with the recruitment of a larger cohort.

Furthermore, the second mapping was not just carried out as a follow-up in 15 out of 18 (83%) patients (in FT analysis, nine out of ten [90%] patients) due to a tumor recurrence and planned reoperation. Thus, it is unclear whether the observed FR was triggered by tumor growth or if it would have happened anyway.

4.5.2. Specific limitations concerning nrTMS-based DTI FT

It is a fact that tractographies become more exact if the results of several algorithms are combined. The reason for this is that, unfortunately, interalgorithm variability is still high (Christidi et al., 2016; Pujol et al., 2015). Recently, an international fiber tracking challenge has shown that most state-of-the-art algorithms produce tractograms that contain 90% of the ground truth bundles. However, at the same time, those algorithms entail many more invalid rather than valid fibers (Maier-Hein et al., 2017).

In this study, we used only one approach: a deterministic DTI tractography algorithm with FACT. This has to be considered a limitation. However, even though the use of another algorithm would have certainly resulted in different fiber numbers, we based our analysis on relations—on relative, not absolute numbers. Therefore, we can exclude the possibility that a systematic error occurred (Ille et al., 2018).

As already mentioned, nrTMS is especially reliable in detecting LNS (Ille et al., 2015a; Krieg et al., 2014b; Picht et al., 2013; Tarapore et al., 2013). However, only LPS are suitable for ROI seeding. As LPS have a lower specificity than LNS (from 28% at an ER ≥5% to 89% at an ER ≥25%), we have to assume that false-positive sites were included and too many fibers were therefore detected (Krieg et al., 2014a). This limitation is of little consequence since we compared not only absolute numbers of fiber quantities but also ratios.

4.6. Conclusion

Overall, this study led us to two key conclusions. First, nrTMS is suitable for the detection of functional reorganization in patients suffering from language-eloquent gliomas. We were able to show with statistical significance that language function initially located inside the tumor area was relocated to different cortical areas over time. This process seems to be highly influenced by the tumor's speed of growth, location, and the presence of functional impairment (Ille et al., 2019).

Second, we found that nrTMS-based DTI FT of single WMPs (IFOF, FAT, SLF/AF) has a high correlation with the patient's status of language function at all examined points in time (Ille et al., 2018).

5. SUMMARY

5.1. English

Preserving the ability to speak and, thus, quality of life is a fundamental mission in the treatment of patients with language eloquent gliomas. Hence, these patients undergo preoperative language mappings to identify regions that need to be spared from resection. We used this mapping data to observe how language networks evolve over the course of this disease. This thesis originated two publications on functional reorganization (FR) of the language network on both cortical and subcortical levels and the associated course of language function.

For the study, *Functional Reorganization of Cortical Language Function in Glioma Patients - A Preliminary Study, by Ille et al., 2019*, we retrospectively recruited 18 patients who were treated for language eloquent gliomas in the neurosurgical department of the Klinikum rechts der Isar MRI TUM, Munich. Every patient had received at least two nrTMS language mappings throughout the treatment. We analyzed this examinational data regarding language-positive sites (LPS) and language-negative sites (LNS). We used the LPS to determine interhemispheric and intrahemispheric dominance ratios, whereas we correlated the change of LNS to the tumor location and, simultaneously, to various patient characteristics. If language function was located near the tumor in the first mapping, we found significantly more LNS in the second mapping, suggesting the migration of language function (Ille et al., 2019).

In the second study, *Language-Eloquent White Matter Pathway Tractography and the Course of Language Function in Glioma Patients, by Ille et al., 2018*, we generated nrTMS-based DTI fiber trackings with applicable data of ten patients from the former sample. In this way, we determined the number of fibers of the entire subcortical language network. We also determined the number of fibers within three single white-matter pathways (WMPs) (the frontal aslant tract, inferior fronto-occipital fascicle, and superior longitudinal and arcuate fascicle) at three different points in time. By comparing these results to the patients' corresponding language function at those times, we found a positive overall correlation between changes in fiber quantity and progression of aphasia (Ille et al., 2018).

In summary, these findings once more reinforce the reliability and broad scope of application in nrTMS diagnostics.

5.2. Deutsch

Eines der obersten Ziele in der Behandlung von Patienten mit spracheloquenten Gliomen ist das Bewahren der Fähigkeit zu Sprechen. Daher werden diese Patienten präoperativen Sprachkartierungen unterzogen um Regionen zu identifizieren, welche während der Resektion geschont werden müssen. Wir haben uns diese Kartierungsdaten zu Nutzen gemacht, um zu beobachten, wie sich die Sprachnetzwerke im Laufe der Erkrankung entwickeln. Diese Doktorarbeit brachte zwei Publikationen über die funktionale Umstrukturierung von Sprachnetzwerken auf kortikaler, sowie auf subkortikaler Ebene und den entsprechenden Verlauf der Sprachfunktion hervor.

Für die Studie, *Functional Reorganization of Cortical Language Function in Glioma Patients - A Preliminary Study, Ille et al., 2019,* rekrutierten wir retrospektiv ein Kollektiv aus 18 Patienten, welche wegen spracheloquenter Gliome in der neurochirurgischen Abteilung des Klinikums rechts der Isar in München behandelt worden waren. Jeder Patient hatte im Verlauf der Behandlung mindestens zwei nrTMS Sprachkartierungen erhalten. Wir analysierten diese Untersuchungsdaten hinsichtlich sprachpositiver (SPA), sowie sprachnegativer Areale (SNA). Die SPA nutzen wir um Inter-, sowie Intrahemispherendominanzverhältnisse zu berechnen, wohingegen wir Veränderungen der SNA mit der Lokalisation des Tumors und gleichzeitig mehreren Patientencharakteristika korrelierten. In jenen Fällen, in welchen, während der ersten Kartierung, Sprachfunktion in der Nähe des Tumors lokalisiert war, fanden wir signifikant mehr SNA in der zweiten Kartierung, was auf eine Abwanderung von Sprachfunktion schließen lässt. (Ille et al., 2019)

In der zweiten Studie, *Language-Eloquent White Matter Pathway Tractography and the Course of Language Function in Glioma Patients*, Ille et al., 2018, erstellten wir nrTMS-basierte DTI Faserbahndarstellungen, mittels geeigneter Daten von zehn Patienten des vorherigen Kollektivs. Auf diese Weise, bestimmten wir die Anzahl an Fasern des gesamten subkortikalen Sprachnetzwerkes, sowie deren Anzahl in drei einzelnen Leitungsbahnen (Frontaler Aslant Trakt, Fasciculus occipitofrontalis inferior, Fasciculus longitudinalis superior und Fasciculus arcuatus) zu drei verschiedenen Zeitpunkten. Indem wir diese Ergebnisse mit der zu jener Zeit entsprechenden Sprachfunktion jedes Patienten in Bezug setzten, fanden wir einen allgemein positiven Zusammenhang zwischen Änderungen in der Faserbahnanzahl und dem Verlauf der Aphasie. (Ille et al., 2018)

Zusammenfassend untermauern diese Erkenntnisse einmal mehr die Zuverlässigkeit und die vielfältigen Einsatzmöglichkeiten der nrTMS Diagnostik.

6. REFERENCES

Abou-Khalil, B., 2007. An update on determination of language dominance in screening for epilepsy surgery: the Wada test and newer noninvasive alternatives. Epilepsia 48, 442-455.

Abraham, W.C., Bear, M.F., 1996. Metaplasticity: the plasticity of synaptic plasticity. Trends Neurosci 19, 126-130.

Aibar-Durán, J., de Quintana-Schmidt, C., Álvarez Holzpafel, M.J., Hernández, F.M., Cortés, C.A., Martínez, G.V., Bertrán, G.C., 2020. Intraoperative Use and Benefits of Tractography in Awake Surgery Patients. World Neurosurg 137, e347-e353.

Barker, A.T., Freeston, I.L., Jalinous, R., Jarratt, J.A., 1987. Magnetic stimulation of the human brain and peripheral nervous system: an introduction and the results of an initial clinical evaluation. Neurosurgery 20, 100-109.

Barker, A.T., Jalinous, R., Freeston, I.L., 1985. Non-invasive magnetic stimulation of human motor cortex. Lancet 1, 1106-1107.

Basser, P.J., Mattiello, J., LeBihan, D., 1994. MR diffusion tensor spectroscopy and imaging. Biophys J 66, 259-267.

Baum, S.H., Martin, R.C., Hamilton, A.C., Beauchamp, M.S., 2012. Multisensory speech perception without the left superior temporal sulcus. Neuroimage 62, 1825-1832.

Beaulieu, C., Allen, P.S., 1994. Determinants of anisotropic water diffusion in nerves. Magn Reson Med 31, 394-400.

Bennett, C.M., Miller, M.B., 2010. How reliable are the results from functional magnetic resonance imaging? Ann N Y Acad Sci 1191, 133-155.

Bennett, E.L., Diamond, M.C., Krech, D., Rosenzweig, M.R., 1996. Chemical and anatomical plasticity of brain. 1964. J Neuropsychiatry Clin Neurosci 8, 459-470.

Berker, E.A., Berker, A.H., Smith, A., 1986. Translation of Broca's 1865 report. Localization of speech in the third left frontal convolution. Arch Neurol 43, 1065-1072.

Broca, P., 1861a. Nouvelle observation d'aphemie produite par une lesion de la troisieme circonvolution frontale. . Bulletins de la Societe d'anatomie 2e serie, 398–407.

Broca, P., 1861b. Perte de la parole, ramollissement chronique et destruction partielle du lobe anterieur gauche. Bull Soc Anthropol 1re serie, 235-238.

Burdach, K.F., 1822. vom Baue und Leben des Gehirns. Dyk Leipzig.

Chang, E.F., Raygor, K.P., Berger, M.S., 2015. Contemporary model of language organization: an overview for neurosurgeons. J Neurosurg 122, 250-261.

Chang, E.F., Wang, D.D., Perry, D.W., Barbaro, N.M., Berger, M.S., 2011. Homotopic organization of essential language sites in right and bilateral cerebral hemispheric dominance. J Neurosurg 114, 893-902.

Charles, P.D., Abou-Khalil, R., Abou-Khalil, B., Wertz, R.T., Ashmead, D.H., Welch, L., Kirshner, H.S., 1994. MRI asymmetries and language dominance. Neurology 44, 2050-2054.

Christidi, F., Karavasilis, E., Samiotis, K., Bisdas, S., Papanikolaou, N., 2016. Fiber tracking: A qualitative and quantitative comparison between four different software tools on the reconstruction of major white matter tracts. Eur J Radiol Open 3, 153-161.

Conway, N., Wildschuetz, N., Moser, T., Bulubas, L., Sollmann, N., Tanigawa, N., Meyer, B., Krieg, S.M., 2017. Cortical plasticity of motor-eloquent areas measured by navigated transcranial magnetic stimulation in patients with glioma. J Neurosurg 127, 981-991.

Corina, D.P., Gibson, E.K., Martin, R., Poliakov, A., Brinkley, J., Ojemann, G.A., 2005. Dissociation of action and object naming: evidence from cortical stimulation mapping. Hum Brain Mapp 24, 1-10.

Darwin, C., 1874. The Descent of Man, and selection in relation to sex. Chicago Rand, McNally and company, Chicago.

De Benedictis, A., Duffau, H., 2011. Brain hodotopy: from esoteric concept to practical surgical applications. Neurosurgery 68, 1709-1723; discussion 1723.

De Witt Hamer, P.C., Robles, S.G., Zwinderman, A.H., Duffau, H., Berger, M.S., 2012. Impact of intraoperative stimulation brain mapping on glioma surgery outcome: a meta-analysis. J Clin Oncol 30, 2559-2565.

Deng, Z.D., Lisanby, S.H., Peterchev, A.V., 2013. Electric field depth-focality tradeoff in transcranial magnetic stimulation: simulation comparison of 50 coil designs. Brain Stimul 6, 1-13.

Desmurget, M., Bonnetblanc, F., Duffau, H., 2007. Contrasting acute and slow-growing lesions: a new door to brain plasticity. Brain 130, 898-914.

Devlin, J.T., Watkins, K.E., 2007. Stimulating language: insights from TMS. Brain 130, 610-622.

Dronkers, N.F., Plaisant, O., Iba-Zizen, M.T., Cabanis, E.A., 2007. Paul Broca's historic cases: high resolution MR imaging of the brains of Leborgne and Lelong. Brain 130, 1432-1441.

Duffau, H., 2006. Brain plasticity: from pathophysiological mechanisms to therapeutic applications. J Clin Neurosci 13, 885-897.

Duffau, H., 2009. Does post-lesional subcortical plasticity exist in the human brain? Neurosci Res 65, 131-135.

Duffau, H., 2013. A new philosophy in surgery for diffuse low-grade glioma (DLGG): oncological and functional outcomes. Neurochirurgie 59, 2-8.

Duffau, H., 2014. The huge plastic potential of adult brain and the role of connectomics: new insights provided by serial mappings in glioma surgery. Cortex 58, 325-337.

Duffau, H., 2018. The error of Broca: From the traditional localizationist concept to a connectomal anatomy of human brain. J Chem Neuroanat 89, 73-81.

Duffau, H., Denvil, D., Capelle, L., 2002. Long term reshaping of language, sensory, and motor maps after glioma resection: a new parameter to integrate in the surgical strategy. J Neurol Neurosurg Psychiatry 72, 511-516.

Duffau, H., Leroy, M., Gatignol, P., 2008a. Cortico-subcortical organization of language networks in the right hemisphere: an electrostimulation study in left-handers. Neuropsychologia 46, 3197-3209.

Duffau, H., Mandonnet, E., 2013. The "onco-functional balance" in surgery for diffuse low-grade glioma: integrating the extent of resection with quality of life. Acta Neurochir (Wien) 155, 951-957.

Duffau, H., Moritz-Gasser, S., Mandonnet, E., 2014. A re-examination of neural basis of language processing: proposal of a dynamic hodotopical model from data provided by brain stimulation mapping during picture naming. Brain Lang 131, 1-10.

Duffau, H., Peggy Gatignol, S.T., Mandonnet, E., Capelle, L., Taillandier, L., 2008b. Intraoperative subcortical stimulation mapping of language pathways in a consecutive series

of 115 patients with Grade II glioma in the left dominant hemisphere. J Neurosurg 109, 461-471.

Elbert, T., Pantev, C., Wienbruch, C., Rockstroh, B., Taub, E., 1995. Increased cortical representation of the fingers of the left hand in string players. Science 270, 305-307.

Elbert, T., Rockstroh, B., 2004. Reorganization of human cerebral cortex: the range of changes following use and injury. Neuroscientist 10, 129-141.

Ettinger, G.J., Leventon, M.E., Grimson, W.E., Kikinis, R., Gugino, L., Cote, W., Sprung, L., Aglio, L., Shenton, M.E., Potts, G., Hernandez, V.L., Alexander, E., 1998. Experimentation with a transcranial magnetic stimulation system for functional brain mapping. Med Image Anal 2, 133-142.

Findlay, A.M., Ambrose, J.B., Cahn-Weiner, D.A., Houde, J.F., Honma, S., Hinkley, L.B., Berger, M.S., Nagarajan, S.S., Kirsch, H.E., 2012. Dynamics of hemispheric dominance for language assessed by magnetoencephalographic imaging. Ann Neurol 71, 668-686.

Fischer, T.M., Blazis, D.E., Priver, N.A., Carew, T.J., 1997. Metaplasticity at identified inhibitory synapses in Aplysia. Nature 389, 860-865.

FitzGerald, D.B., Cosgrove, G.R., Ronner, S., Jiang, H., Buchbinder, B.R., Belliveau, J.W., Rosen, B.R., Benson, R.R., 1997. Location of language in the cortex: a comparison between functional MR imaging and electrocortical stimulation. AJNR Am J Neuroradiol 18, 1529-1539.

Flor, H., Elbert, T., Knecht, S., Wienbruch, C., Pantev, C., Birbaumer, N., Larbig, W., Taub, E., 1995. Phantom-limb pain as a perceptual correlate of cortical reorganization following arm amputation. Nature 375, 482-484.

Frey, D., Schilt, S., Strack, V., Zdunczyk, A., Rosler, J., Niraula, B., Vajkoczy, P., Picht, T., 2014. Navigated transcranial magnetic stimulation improves the treatment outcome in patients with brain tumors in motor eloquent locations. Neuro Oncol 16, 1365-1372.

Fridriksson, J., Yourganov, G., Bonilha, L., Basilakos, A., Den Ouden, D.B., Rorden, C., 2016. Revealing the dual streams of speech processing. Proc Natl Acad Sci U S A 113, 15108-15113.

Fritsch, G.H., E., 1870. Ueber die elektrische Erregbarkeit des Grosshirns. G. Eichler, Berlin.

Fujii, M., Maesawa, S., Ishiai, S., Iwami, K., Futamura, M., Saito, K., 2016. Neural Basis of Language: An Overview of An Evolving Model. Neurol Med Chir (Tokyo) 56, 379-386.

Fujii, M., Maesawa, S., Motomura, K., Futamura, M., Hayashi, Y., Koba, I., Wakabayashi, T., 2015. Intraoperative subcortical mapping of a language-associated deep frontal tract connecting the superior frontal gyrus to Broca's area in the dominant hemisphere of patients with glioma. J Neurosurg 122, 1390-1396.

Giussani, C., Roux, F.E., Ojemann, J., Sganzerla, E.P., Pirillo, D., Papagno, C., 2010. Is preoperative functional magnetic resonance imaging reliable for language areas mapping in brain tumor surgery? Review of language functional magnetic resonance imaging and direct cortical stimulation correlation studies. Neurosurgery 66, 113-120.

Haglund, M.M., Berger, M.S., Shamseldin, M., Lettich, E., Ojemann, G.A., 1994. Cortical localization of temporal lobe language sites in patients with gliomas. Neurosurgery 34, 567-576; discussion 576.

Hamberger, M.J., 2007. Cortical language mapping in epilepsy: a critical review. Neuropsychol Rev 17, 477-489.

Hauck, T., Tanigawa, N., Probst, M., Wohlschlaeger, A., Ille, S., Sollmann, N., Maurer, S., Zimmer, C., Ringel, F., Meyer, B., Krieg, S.M., 2015. Stimulation frequency determines the distribution of language positive cortical regions during navigated transcranial magnetic brain stimulation. BMC Neurosci 16, 5.

Hayashi, Y., Nakada, M., Kinoshita, M., Hamada, J., 2014. Functional reorganization in the patient with progressing glioma of the pure primary motor cortex: a case report with special reference to the topographic central sulcus defined by somatosensory-evoked potential. World Neurosurg 82, 536.e531-534.

Hebb, D.O., 1949. The Organization of Behavior. Wiley & Sons, New York.

Hervey-Jumper, S.L., Berger, M.S., 2016. Maximizing safe resection of low- and high-grade glioma. J Neurooncol 130, 269-282.

Hickok, G., Poeppel, D., 2004. Dorsal and ventral streams: a framework for understanding aspects of the functional anatomy of language. Cognition 92, 67-99.

Hickok, G., Poeppel, D., 2007. The cortical organization of speech processing. Nat Rev Neurosci 8, 393-402.

Huber, W., Weniger, D., Poeck, K., Willmes, K., 1980. [The Aachen Aphasia Test Rationale and construct validity (author's transl)]. Nervenarzt 51, 475-482.

Ille, S., Engel, L., Albers, L., Schroeder, A., Kelm, A., Meyer, B., Krieg, S.M., 2019. Functional Reorganization of Cortical Language Function in Glioma Patients-A Preliminary Study. Front Oncol 9, 446.

Ille, S., Engel, L., Kelm, A., Meyer, B., Krieg, S.M., 2018. Language-Eloquent White Matter Pathway Tractography and the Course of Language Function in Glioma Patients. Front Oncol 8, 572.

Ille, S., Kulchytska, N., Sollmann, N., Wittig, R., Beurskens, E., Butenschoen, V.M., Ringel, F., Vajkoczy, P., Meyer, B., Picht, T., Krieg, S.M., 2016. Hemispheric language dominance measured by repetitive navigated transcranial magnetic stimulation and postoperative course of language function in brain tumor patients. Neuropsychologia 91, 50-60.

Ille, S., Schwendner, M., Zhang, W., Schroeder, A., Meyer, B., Krieg, S.M., 2021. Tractography for Subcortical Resection of Gliomas Is Highly Accurate for Motor and Language Function: ioMRI-Based Elastic Fusion Disproves the Severity of Brain Shift. Cancers (Basel) 13.

Ille, S., Sollmann, N., Hauck, T., Maurer, S., Tanigawa, N., Obermueller, T., Negwer, C., Droese, D., Boeckh-Behrens, T., Meyer, B., Ringel, F., Krieg, S.M., 2015a. Impairment of preoperative language mapping by lesion location: a functional magnetic resonance imaging, navigated transcranial magnetic stimulation, and direct cortical stimulation study. J Neurosurg 123, 314-324.

Ille, S., Sollmann, N., Hauck, T., Maurer, S., Tanigawa, N., Obermueller, T., Negwer, C., Droese, D., Zimmer, C., Meyer, B., Ringel, F., Krieg, S.M., 2015b. Combined noninvasive language mapping by navigated transcranial magnetic stimulation and functional MRI and its comparison with direct cortical stimulation. J Neurosurg 123, 212-225.

Ius, T., Angelini, E., Thiebaut de Schotten, M., Mandonnet, E., Duffau, H., 2011. Evidence for potentials and limitations of brain plasticity using an atlas of functional resectability of WHO grade II gliomas: towards a "minimal common brain". Neuroimage 56, 992-1000.

James, W., 1890. The Principles of Psychology. Vol. 1.

Keidel, J.L., Welbourne, S.R., Lambon Ralph, M.A., 2010. Solving the paradox of the equipotential and modular brain: a neurocomputational model of stroke vs. slow-growing glioma. Neuropsychologia 48, 1716-1724.

Kelm, A., Sollmann, N., Ille, S., Meyer, B., Ringel, F., Krieg, S.M., 2017. Resection of Gliomas with and without Neuropsychological Support during Awake Craniotomy-Effects on Surgery and Clinical Outcome. Front Oncol 7, 176.

Knecht, S., Drager, B., Deppe, M., Bobe, L., Lohmann, H., Floel, A., Ringelstein, E.B., Henningsen, H., 2000. Handedness and hemispheric language dominance in healthy humans. Brain 123 Pt 12, 2512-2518.

Kong, N.W., Gibb, W.R., Tate, M.C., 2016. Neuroplasticity: Insights from Patients Harboring Gliomas. Neural Plast 2016, 2365063.

Krieg, S., 2017. Navigated Transcranial Magnetic Stimulation in Neurosurgery.

Krieg, S.M., Lioumis, P., Makela, J.P., Wilenius, J., Karhu, J., Hannula, H., Savolainen, P., Lucas, C.W., Seidel, K., Laakso, A., Islam, M., Vaalto, S., Lehtinen, H., Vitikainen, A.M., Tarapore, P.E., Picht, T., 2017. Protocol for motor and language mapping by navigated TMS in patients and healthy volunteers; workshop report. Acta Neurochir (Wien) 159, 1187-1195.

Krieg, S.M., Shiban, E., Buchmann, N., Gempt, J., Foerschler, A., Meyer, B., Ringel, F., 2012. Utility of presurgical navigated transcranial magnetic brain stimulation for the resection of tumors in eloquent motor areas. J Neurosurg 116, 994-1001.

Krieg, S.M., Sollmann, N., Hauck, T., Ille, S., Foerschler, A., Meyer, B., Ringel, F., 2013. Functional language shift to the right hemisphere in patients with language-eloquent brain tumors. PLoS One 8, e75403.

Krieg, S.M., Sollmann, N., Hauck, T., Ille, S., Meyer, B., Ringel, F., 2014a. Repeated mapping of cortical language sites by preoperative navigated transcranial magnetic stimulation compared to repeated intraoperative DCS mapping in awake craniotomy. BMC Neurosci 15, 20.

Krieg, S.M., Sollmann, N., Tanigawa, N., Foerschler, A., Meyer, B., Ringel, F., 2016. Cortical distribution of speech and language errors investigated by visual object naming and navigated transcranial magnetic stimulation. Brain Struct Funct 221, 2259-2286.

Krieg, S.M., Tarapore, P.E., Picht, T., Tanigawa, N., Houde, J., Sollmann, N., Meyer, B., Vajkoczy, P., Berger, M.S., Ringel, F., Nagarajan, S., 2014b. Optimal timing of pulse onset for language mapping with navigated repetitive transcranial magnetic stimulation. Neuroimage 100, 219-236.

Liepert, J., Tegenthoff, M., Malin, J.P., 1995. Changes of cortical motor area size during immobilization. Electroencephalogr Clin Neurophysiol 97, 382-386.

Lioumis, P., Zhdanov, A., Makela, N., Lehtinen, H., Wilenius, J., Neuvonen, T., Hannula, H., Deletis, V., Picht, T., Makela, J.P., 2012. A novel approach for documenting naming errors induced by navigated transcranial magnetic stimulation. J Neurosci Methods 204, 349-354.

Magee, J.A., Pender, N.P., Abrahams, S., Thornton, J., Delanty, N., Fortune, G.M., 2012. A comparison of propofol and amobarbital for use in the Wada test. Seizure 21, 399-401.

Maier-Hein, K.H., Neher, P.F., Houde, J.C., Côté, M.A., Garyfallidis, E., Zhong, J., Chamberland, M., Yeh, F.C., Lin, Y.C., Ji, Q., Reddick, W.E., Glass, J.O., Chen, D.Q., Feng, Y., Gao, C., Wu, Y., Ma, J., He, R., Li, Q., Westin, C.F., Deslauriers-Gauthier, S., González, J.O.O., Paquette, M., St-Jean, S., Girard, G., Rheault, F., Sidhu, J., Tax, C.M.W., Guo, F., Mesri, H.Y., Dávid, S., Froeling, M., Heemskerk, A.M., Leemans, A., Boré, A., Pinsard, B., Bedetti, C., Desrosiers, M., Brambati, S., Doyon, J., Sarica, A., Vasta, R., Cerasa, A., Quattrone, A., Yeatman, J., Khan, A.R., Hodges, W., Alexander, S., Romascano, D., Barakovic, M., Auría, A., Esteban, O., Lemkaddem, A., Thiran, J.P., Cetingul, H.E., Odry, B.L., Mailhe, B., Nadar, M.S., Pizzagalli, F., Prasad, G., Villalon-Reina, J.E., Galvis, J., Thompson, P.M., Requejo, F.S., Laguna, P.L., Lacerda, L.M., Barrett, R., Dell'Acqua, F., Catani, M., Petit, L., Caruyer, E., Daducci, A., Dyrby, T.B., Holland-Letz, T., Hilgetag, C.C., Stieltjes, B., Descoteaux, M., 2017. The challenge of mapping the human connectome based on diffusion tractography. Nat Commun 8, 1349.

Mandonnet, E., Duffau, H., 2018. An attempt to conceptualize the individual onco-functional balance: Why a standardized treatment is an illusion for diffuse low-grade glioma patients. Crit Rev Oncol Hematol 122, 83-91.

Martino, J., Taillandier, L., Moritz-Gasser, S., Gatignol, P., Duffau, H., 2009. Re-operation is a safe and effective therapeutic strategy in recurrent WHO grade II gliomas within eloquent areas. Acta Neurochir (Wien) 151, 427-436; discussion 436.

Merton, P.A., Morton, H.B., 1980. Stimulation of the cerebral cortex in the intact human subject. Nature 285, 227.

Milian, M., Tatagiba, M., Feigl, G.C., 2014. Patient response to awake craniotomy - a summary overview. Acta Neurochir (Wien) 156, 1063-1070.

Moritz-Gasser, S., Herbet, G., Duffau, H., 2013. Mapping the connectivity underlying multimodal (verbal and non-verbal) semantic processing: a brain electrostimulation study. Neuropsychologia 51, 1814-1822.

Mühlnickel, W., Elbert, T., Taub, E., Flor, H., 1998. Reorganization of auditory cortex in tinnitus. Proc Natl Acad Sci U S A 95, 10340-10343.

Negwer, C., 2018. Function-based DTI fiber tracking using repetitive transcranial magnetic stimulation for language-relevant subcortical fiber tracts: feasibility and application of a novel technique in patients with left-sided perisylvian brain tumors., Fakultät für Medizin. Technische Universität München.

Negwer, C., Ille, S., Hauck, T., Sollmann, N., Maurer, S., Kirschke, J.S., Ringel, F., Meyer, B., Krieg, S.M., 2017a. Visualization of subcortical language pathways by diffusion tensor imaging fiber tracking based on rTMS language mapping. Brain Imaging Behav 11, 899-914.

Negwer, C., Sollmann, N., Ille, S., Hauck, T., Maurer, S., Kirschke, J.S., Ringel, F., Meyer, B., Krieg, S.M., 2017b. Language pathway tracking: comparing nTMS-based DTI fiber tracking with a cubic ROIs-based protocol. J Neurosurg 126, 1006-1014.

Ogawa, S., Lee, T.M., Kay, A.R., Tank, D.W., 1990. Brain magnetic resonance imaging with contrast dependent on blood oxygenation. Proc Natl Acad Sci U S A 87, 9868-9872.

Ojemann, G.A., Whitaker, H.A., 1978. Language localization and variability. Brain Lang 6, 239-260.

Oldfield, R.C., 1971. The assessment and analysis of handedness: the Edinburgh inventory. Neuropsychologia 9, 97-113.

Pascual-Leone, A., Amedi, A., Fregni, F., Merabet, L.B., 2005. The plastic human brain cortex. Annu Rev Neurosci 28, 377-401.

Pascual-Leone, A., Gates, J.R., Dhuna, A., 1991. Induction of speech arrest and counting errors with rapid-rate transcranial magnetic stimulation. Neurology 41, 697-702.

Pascual-Leone, A., Torres, F., 1993. Plasticity of the sensorimotor cortex representation of the reading finger in Braille readers. Brain 116 (Pt 1), 39-52.

Pascual-Leone, A., Walsh, V., Rothwell, J., 2000. Transcranial magnetic stimulation in cognitive neuroscience--virtual lesion, chronometry, and functional connectivity. Curr Opin Neurobiol 10, 232-237.

Penfield, W., Boldrey, E., 1937. Somatic Motor and Sensory Representation in the Cerebral Cortex of Man as Studied by Electrical Stimulation Brain 60, 389-443.

Penfield, W., Rasmussen, T., 1949. Vocalization and arrest of speech. Arch Neurol Psychiatry 61, 21-27.

Penfield, W., Roberts, L., 1959. Speech and brain mechanisms. Princeton University Press, Princeton, NJ, US.

Petrovich Brennan, N.M., Whalen, S., de Morales Branco, D., O'Shea J, P., Norton, I.H., Golby, A.J., 2007. Object naming is a more sensitive measure of speech localization than number counting: Converging evidence from direct cortical stimulation and fMRI. Neuroimage 37 Suppl 1, S100-108.

Picart, T., Herbet, G., Moritz-Gasser, S., Duffau, H., 2019. Iterative Surgical Resections of Diffuse Glioma With Awake Mapping: How to Deal With Cortical Plasticity and Connectomal Constraints? Neurosurgery 85, 105-116.

Picht, T., Kombos, T., Gramm, H.J., Brock, M., Suess, O., 2006. Multimodal protocol for awake craniotomy in language cortex tumour surgery. Acta Neurochir (Wien) 148, 127-137; discussion 137-128.

Picht, T., Krieg, S.M., Sollmann, N., Rosler, J., Niraula, B., Neuvonen, T., Savolainen, P., Lioumis, P., Makela, J.P., Deletis, V., Meyer, B., Vajkoczy, P., Ringel, F., 2013. A comparison of language mapping by preoperative navigated transcranial magnetic stimulation and direct cortical stimulation during awake surgery. Neurosurgery 72, 808-819.

Pons, T.P., Garraghty, P.E., Ommaya, A.K., Kaas, J.H., Taub, E., Mishkin, M., 1991. Massive cortical reorganization after sensory deafferentation in adult macaques. Science 252, 1857-1860.

Pujol, S., Wells, W., Pierpaoli, C., Brun, C., Gee, J., Cheng, G., Vemuri, B., Commowick, O., Prima, S., Stamm, A., Goubran, M., Khan, A., Peters, T., Neher, P., Maier-Hein, K.H., Shi, Y., Tristan-Vega, A., Veni, G., Whitaker, R., Styner, M., Westin, C.F., Gouttard, S., Norton, I., Chauvin, L., Mamata, H., Gerig, G., Nabavi, A., Golby, A., Kikinis, R., 2015. The DTI Challenge: Toward Standardized Evaluation of Diffusion Tensor Imaging Tractography for Neurosurgery. J Neuroimaging 25, 875-882.

Raffa, G., Bährend, I., Schneider, H., Faust, K., Germanò, A., Vajkoczy, P., Picht, T., 2016. A Novel Technique for Region and Linguistic Specific nTMS-based DTI Fiber Tracking of Language Pathways in Brain Tumor Patients. Front Neurosci 10, 552.

Rauschecker, J.P., Scott, S.K., 2009. Maps and streams in the auditory cortex: nonhuman primates illuminate human speech processing. Nat Neurosci 12, 718-724.

Robles, S.G., Gatignol, P., Lehericy, S., Duffau, H., 2008. Long-term brain plasticity allowing a multistage surgical approach to World Health Organization Grade II gliomas in eloquent areas. J Neurosurg 109, 615-624.

Rosler, J., Niraula, B., Strack, V., Zdunczyk, A., Schilt, S., Savolainen, P., Lioumis, P., Makela, J., Vajkoczy, P., Frey, D., Picht, T., 2014. Language mapping in healthy volunteers and brain tumor patients with a novel navigated TMS system: evidence of tumor-induced plasticity. Clin Neurophysiol 125, 526-536.

Rossi, S., Hallett, M., Rossini, P.M., Pascual-Leone, A., 2009. Safety, ethical considerations, and application guidelines for the use of transcranial magnetic stimulation in clinical practice and research. Clin Neurophysiol 120, 2008-2039.

Rossini, P.M., Burke, D., Chen, R., Cohen, L.G., Daskalakis, Z., Di Iorio, R., Di Lazzaro, V., Ferreri, F., Fitzgerald, P.B., George, M.S., Hallett, M., Lefaucheur, J.P., Langguth, B., Matsumoto, H., Miniussi, C., Nitsche, M.A., Pascual-Leone, A., Paulus, W., Rossi, S., Rothwell, J.C., Siebner, H.R., Ugawa, Y., Walsh, V., Ziemann, U., 2015. Non-invasive electrical and magnetic stimulation of the brain, spinal cord, roots and peripheral nerves: Basic principles and procedures for routine clinical and research application. An updated report from an I.F.C.N. Committee. Clin Neurophysiol 126, 1071-1107.

Ruohonen, J., Karhu, J., 2010. Navigated transcranial magnetic stimulation. Neurophysiol Clin 40, 7-17.

Sanai, N., Mirzadeh, Z., Berger, M.S., 2008. Functional outcome after language mapping for glioma resection. N Engl J Med 358, 18-27.

Sollmann, N., Tanigawa, N., Ringel, F., Zimmer, C., Meyer, B., Krieg, S.M., 2014. Language and its right-hemispheric distribution in healthy brains: an investigation by repetitive transcranial magnetic stimulation. Neuroimage 102 Pt 2, 776-788.

Sollmann, N., Wildschuetz, N., Kelm, A., Conway, N., Moser, T., Bulubas, L., Kirschke, J.S., Meyer, B., Krieg, S.M., 2018. Associations between clinical outcome and navigated transcranial magnetic stimulation characteristics in patients with motor-eloquent brain lesions: a combined navigated transcranial magnetic stimulation-diffusion tensor imaging fiber tracking approach. J Neurosurg 128, 800-810.

Southwell, D.G., Hervey-Jumper, S.L., Perry, D.W., Berger, M.S., 2016. Intraoperative mapping during repeat awake craniotomy reveals the functional plasticity of adult cortex. J Neurosurg 124, 1460-1469.

Sperry, R.W., 1974. Lateral specialization in the surgically separated hemispheres. . The Neurosciences. 3rd Study Program Vol. 3, pp. 5- 19.

Szaflarski, J.P., Binder, J.R., Possing, E.T., McKiernan, K.A., Ward, B.D., Hammeke, T.A., 2002. Language lateralization in left-handed and ambidextrous people: fMRI data. Neurology 59, 238-244.

Szalisznyo, K., Silverstein, D.N., Duffau, H., Smits, A., 2013. Pathological neural attractor dynamics in slowly growing gliomas supports an optimal time frame for white matter plasticity. PLoS One 8, e69798.

Talacchi, A., Santini, B., Casagrande, F., Alessandrini, F., Zoccatelli, G., Squintani, G.M., 2013. Awake surgery between art and science. Part I: clinical and operative settings. Funct Neurol 28, 205-221.

Tarapore, P.E., Findlay, A.M., Honma, S.M., Mizuiri, D., Houde, J.F., Berger, M.S., Nagarajan, S.S., 2013. Language mapping with navigated repetitive TMS: proof of technique and validation. Neuroimage 82, 260-272.

Toga, A.W., Thompson, P.M., 2003. Mapping brain asymmetry. Nat Rev Neurosci 4, 37-48.

Tremblay, P., Dick, A.S., 2016. Broca and Wernicke are dead, or moving past the classic model of language neurobiology. Brain Lang 162, 60-71.

Turrigiano, G.G., Nelson, S.B., 2004. Homeostatic plasticity in the developing nervous system. Nat Rev Neurosci 5, 97-107.

Ueno, S., Tashiro, T., Harada, K., 1988. Localized stimulation of neural tissues in the brain by means of a paired configuration of time-varying magnetic fields. Journal of Applied Physics 64, 5862-5864.

Wada, J., Rasmussen, T., 2007. Intracarotid injection of sodium amytal for the lateralization of cerebral speech dominance. 1960. J Neurosurg 106, 1117-1133.

Wernicke, C., 1874. Der aphasische Symptomencomplex. Eine psychologische Studie auf anatomischer Basis. . M. Cohn & Weigert, Breslau.

Whitaker, H.A., Etlinger, S.C., 1993. Theodor Meynert's contribution to classical 19th century aphasia studies. Brain Lang 45, 560-571.

Wilkins, R.H., Brody, I.A., 1970. Wernicke's sensory aphasia. Arch Neurol 22, 279-282.

Zanatta, A., Cherici, C., Bargoni, A., Buzzi, S., Cani, V., Mazzarello, P., Zampieri, F., 2018. Vincenzo Malacarne (1744-1816) and the First Description of the Human Cerebellum. Cerebellum 17, 461-464.

7. ABBREVIATIONS

3D	Three-dimensional
A	Anterior tumors
AA	Astrocytoma
AAT	Aachener Aphasia Test
aHDR	Anterior hemispheric dominance ratio
AED	Anti-epileptic-drugs
aER	Error rate anterior perisylvian regions
AF	Arcuate fascicle
aHDR	Anterior hemispheric dominance
aMTG	Anterior middle temporal gyrus
anG	Angular gyrus
aSMG	Anterior supramarginal gyrus
aSTG	Anterior superior temporal gyrus
BOLD	Blood oxygen level-dependent
CPS	Cortical parcellation system
DA	Diffuse astrocytoma
DES	Direct electrical stimulation
DICOM	Digital Imaging and Communications in Medicine
DTI	Diffusion tensor imaging
DWI	Diffusion-weighed MRI
EHI	Edinburgh Handedness Inventory
EMG	Electromyography
EOR	Extent of resection
ER	Error rate
FA	Fractional anisotropy
FACT	Fiber Assignment by Continuous Tracking
FAT	Frontal aslant tract
fMRI	Functional magnetic resonance imaging
FR	Functional Reorganization
FT	Fiber tracking
GBM	Glioblastoma
HDR	Hemispheric Dominance Ratio
ID	Patient identification number
IDH	Isocitrate dehydrogenase
IDR	Intrahemispheric dominace ratio

IFOF	Inferior frontooccipital fasclicle
IHR	Intrahemispheric dominance ratio
ILF	Inferior Longitudinal Fasclicle
LNS	Language negative site
LPS	Language positive site
LQ	Laterality quotient
LTD	Long-term depression
LTP	Long-term potentiation
MEG	Magnetoencephalography
MEP	Motor evoked potentials
MFL	Minimum fiber length
mMFG	Middle middle frontal gyrus
mMTG	Middle middle temporal gyrus
MP-RAGE	Magnetization-prepared rapid gradient-echo sequence
MRI	Magnetic resonance imaging
mSTG	Middle superior temporal gyrus
NPV	Negative predictive value
nrTMS	Navigated repetitive Transcranial Magnetic Stimulation
nTMS	Navigated transcranial magnetic stimulation
OD	Oligodendroglioma
opIFG	Opercular inferior frontal gyrus
P	Posterior tumors
pER	Error rate of posterior perisylvian regions
pHDR	Posterior hemispheric dominance ratio
pMFG	Posterior middle frontal gyrus
POD5-1	Five days postoperatively after the first surgery
POD5-2	Five days postoperatively after the second surgery
POM3-1	Three months postoperatively after the first surgery
POM3-2	Three months postoperatively after the second surgery
PRE-1	Preoperatively to the first surgery
PRE-2	Preoperatively to the second surgery
pSMG	Posterior supramarginal gyrus
pSTG	Posterior superior temporal gyrus
RMT	Resting motor threshold
rTMS	Rapid rate TMS
ROI	Region of interest
SLF	Superior Longitudinal Fascicle

SNA	Sprachnegatives Areal
SPA	Sprachpositives Areal
STG	Superior temporal gyrus
TA	Tumor area
TIVA	Total intravenous anaesthesia
TMS	Transcranial magnetic stimulation
trIFG	Trinangular inferior frontal gyrus
UF	Uncinate fascicle
vPrG	Ventral pre-central gyrus
WOT	Area without tumor
WMP	White-matter pathways

8. ACKNOWLEDGEMENTS

Zunächst möchte ich meinem Doktorvater Prof. Dr. med. Sandro Krieg meinen Dank aussprechen. Ohne seine Anregungen, Kritik und Unterstützung hätte diese Arbeit nie zustande kommen können.

Außerdem möchte ich mich herzlichst bei meinem Betreuer PD Dr. med. Sebastian Ille bedanken, der mir stets mit Rat, Tat und Hilfestellung zur Seite stand.

Des Weiteren, ein ganz herzliches Dankeschön an alle aktuellen und ehemaligen Mitglieder der TMS-Gruppe. Ein besonderer Dank gilt Axel Schröder, der mich jederzeit in allen praktischen Fragen unterstützte. In unserer Arbeitsgruppe durfte ich über die Jahre sehr viel Kollegialität und Hilfsbereitschaft erfahren.

Auch gilt mein tiefster Dank meiner Familie, insbesondere meiner Mutter Sibylle, die mich seit jeher in meiner beruflichen Laufbahn und allen weiteren Lebenslagen unterstützt. Ohne sie wäre diese Dissertation nicht möglich gewesen.

Zuletzt möchte ich Martin danken, der mich besonders in den letzten Phasen meiner Arbeit motivierte und fachlich, praktisch und emotional immer für mich da war.

9. PUBLICATIONS

Original papers

Ille, S., Engel, L., Kelm, A., Meyer, B., Krieg, S. M.

Language-Eloquent White Matter Pathway Tractography and the Course of Language Function in Glioma Patients.

Frontiers of Oncology 2018 Dec 24; DOI: 10.3389/fonc.2018.00572

Ille, S., Engel, L., Albers, L., Schroeder, A., Kelm, A., Meyer, B., Krieg, S. M.

Functional Reorganization of Cortical Language Function in Glioma Patients-A Preliminary Study

Frontiers of Oncology 2019 Jun 25; DOI: 10.3389/fonc.2019.00446